

C–H Bond Functionalization under  
Electrochemical Flow ConditionsTamlal Pokhrel,<sup>[a]</sup> Bijaya B. K.,<sup>[a]</sup> Ramesh Giri,<sup>[a]</sup> Achyut Adhikari,<sup>[a]</sup> and Nisar Ahmed\*<sup>[b]</sup>

**Abstract:** Electrochemical C–H functionalization is a rapidly growing area of interest in organic synthesis. To achieve maximum atom economy, the flow electrolysis process is more sustainable. This allows shorter reaction times, safer working environments, and better selectivities. Using this technology, the problem of overoxidation can be reduced and less emergence of side products or no side products are possible. Flow electro-reactors provide high surface-to-volume ratios and contain electrodes that are closely spaced where the diffusion layers overlap to give the desired product, electrochemical processes can now be managed without the need for a deliberately added supporting electrolyte. Considering the importance of flow electrochemical C–H functionalization, a comprehensive review is presented. Herein, we summarize flow electrolysis for the construction of C–C and C–X (X=O, N, S, and I) bonds formation. Also, benzylic oxidation and access to biologically active molecules are discussed.

**Keywords:** C–H bonds activation, Flow electrochemistry, Microreactors, Green and sustainable chemistry, Reaction engineering

## 1. Introduction

Organic compounds have vast structural diversity that consists of chains or rings of carbon atoms decorated with a large number of hydrogen atoms.<sup>[1]</sup> Organic synthesis is the process of constructing new organic molecules either by introducing new desirable functional groups or transforming the functional group. Functionalization of the particular C–H bond is omnipresent in the organic synthesis. Selective functionalization of C–H initiates the organic synthesis reaction, although the functionalization of the C–H bond has been recognized as

a challenging task in organic synthesis. C–H bond functionalization has gained attention as a new and promising area for the construction of C–C and C–X (X=O, N, S, I, etc.) bonds. C–H bond functionalization strategy would allow the versatile transformation in the organic synthesis.<sup>[2]</sup> Due to the presence of strong C(sp<sup>3</sup>)–H and C(sp<sup>3</sup>)–C(sp<sup>3</sup>) bonds, alkanes are the least reactive organic molecules.<sup>[3]</sup> Many methods are derived to activate the C–H bond of alkane. The classical method carries out functionalization of the non-reactive C–H bond by the formation of free radicals.<sup>[4]</sup> There has been explosive growth in the development of methods for C–H bond functionalization. There are many verified and simple techniques available to operate the stereoselective and site-selective functionalization in organic synthesis.<sup>[5]</sup> Enzyme catalysis, organometallic catalysis, and electrochemical approaches for the functional group introduce methods to invigorate the application of organic synthesis.<sup>[6–8]</sup>

Mostly, five methods of C–H bond functionalization are well known: (i) stepwise radical pathways,<sup>[9]</sup> (ii) carbene/nitrene insertion mechanism,<sup>[10]</sup> (iii) metal-mediated C–H bond activation,<sup>[11,12]</sup> (iv) enzymatic functionalization,<sup>[6]</sup> and (v) photochemical method.<sup>[13]</sup> Alkane transformation by using radical pathways of carbene/nitrene insertion is somewhat

[a] T. Pokhrel, B. B. K., R. Giri, A. Adhikari

Central Department of Chemistry, Tribhuvan University, Kirtipur 44618, Kathmandu, Nepal

[b] N. Ahmed

School of Chemistry, Cardiff University, Main Building, Park Place, Cardiff, CF10 3AT, United Kingdom  
E-mail: AhmedN14@cardiff.ac.uk

© 2022 The Authors. Published by The Chemical Society of Japan & Wiley-VCH GmbH. This is an open access article under the terms of the Creative Commons Attribution Non-Commercial License, which permits use, distribution and reproduction in any medium, provided the original work is properly cited and is not used for commercial purposes.

applicable to small-scale production. Using highly reactive radicals in the reaction is relatively expensive and less applicable for the functionalization of the linear alkane.<sup>[3]</sup> Transition metal-catalyzed C–H bond functionalization is a relatively cost-effective and environment-friendly technique, besides many advantages, this method also suffers from very

low efficiency and less selectivity.<sup>[3,14]</sup> Electro-organic synthesis is the best alternative to traditional synthetic procedures for organic synthesis because it uses clean electrons from electrodes placed at their nearest proximity instead of particular reductants or oxidants.<sup>[15–17]</sup> The relatively small-scale production of important chemicals can be performed in a stirred tank



Nisar Ahmed obtained his Ph.D. in organic chemistry (2012) under Brain Korea BK21 fellowship working in the group of Prof. Kwang S. Kim (POST-ECH, Korea). Then, he moved to the University of Zurich, Switzerland (2013) for a postdoctoral stay with a Novartis fellowship. Subsequently (2015), he joined the University of Bristol as a research associate. He started his independent research in 2017 at the School of Chemistry, Cardiff University, United Kingdom with Marie Curie COFUND fellowship as Sêr Cymru Fellow. Subsequently, he was appointed Faculty in molecular synthesis (organic chemistry) and Research Fellow-EPSRC Investigator (UKRI) at Cardiff School of Chemistry, Cardiff University. He is also an Adjunct faculty at HEJ Research Institute of Chemistry, ICCBS since 2018. His fields of research include value-added chemicals synthesis using modern synthetic tools (electrocatalysis, photoelectrocatalysis, sonoelectrochemistry, flow technology, digital & automation chemistry) and molecular recognition of biomolecules using fluorescent probes (supramolecular chemistry).



Tamlal Pokhrel obtained his master's degree in Organic Chemistry in 2021 at Tribhuvan University. He completed the master's degree under the supervision of Assoc. Prof. Dr. Achyut Adhikari. During this time, he spent 9 months as a research intern in the Department of Plant Resources, Kathmandu. His major research interests are Natural products, Organic-synthesis, and Nanoparticles.



Bijaya B.K. obtained his MSc in chemistry with a major in organic chemistry from the Central Department of Chemistry, Tribhuvan University, Nepal. During his Master's degree, he has studied the chemical composition of human gallstones and investigated the in vitro dissolution of human gallstones. He was awarded Master Dissertation Research Grant from the National Youth Council, Government of Nepal. During his bachelor's degree, as project work, he has analyzed the quality of cooking oil. His major research area includes organic synthesis, natural product chemistry, biochemistry, and analytical chemistry.



Ramesh Giri has completed his Master's degree in chemistry taking organic chemistry as a major from the Central Department of Chemistry, Tribhuvan University, Nepal. During his Master's degree, he synthesized fine size silver nanoparticles from *Terminalia chebula* Retz. and investigate biological activities, and also awarded with a Master thesis grant provided by University Grants Commission (UGC), Nepal. His major research area is Organic synthesis, Nanotechnology, Analytical chemistry, and Natural product chemistry.



Dr. Achyut Adhikari was born in Palpa, Nepal in 1980. He obtained his Ph. D. degree from the International Center for Chemical and Biological Sciences, University of Karachi, Pakistan, in 2010. He was an Assistant Professor between 2012–2017 in the same Institution. Dr. Adhikari is presently working as an Associate Professor in the Central Department of Chemistry, Tribhuvan University, Nepal. His areas of research interest are structural and bio-organic chemistry. He has published over 100 articles in international journals.

batch reactor. However, applications of such reactors in large-scale production are limited by inefficient control over reaction parameters such as temperature, stirring efficiency, and pressure. For the first time, Kolbe studied the electrolysis of organic compounds in 1840s.<sup>[18]</sup> After this achievement, more researchers were concerned about electro-organic synthesis. C–H functionalization strategies have developed enormously in the last decade. Electrochemical C–H activation has been considered as a powerful strategy that uses electricity in place of non-eco-friendly chemical transformation. The continuous-flow method is a more reliable and easily optimizable procedure in preference to the traditionally used batch procedure. The continuous-flow procedure also brings numerous advantages in the pharmaceutical industry, but the implementation is not so easy.<sup>[19]</sup>

For electrochemical synthetic transformation, there are different strategies such as batch electrochemistry,<sup>[20]</sup> photo-electrocatalysis,<sup>[21]</sup> metallo-electrocatalysis,<sup>[22]</sup> organo-electrocatalysis,<sup>[23]</sup> etc. To reduce the use of expensive reagents, to increase the effectiveness and productivity, all the electrochemical methods are based on simple electron transfer from the electrode to the substrate or vice versa. There are three different scenarios for the electron transfer from the electrode to the substrate (Figure 1).<sup>[24]</sup> Electrochemistry substituted the conventional chemical oxidizing and reducing agents by

inexpensive, renewable, and inherently benign electrolysis techniques.<sup>[25]</sup> The electrochemical reaction involves the electron transfer at the electrode-electrolyte interface.<sup>[26]</sup> Kolbe<sup>[27]</sup> pioneered the field of electro-organic synthesis in the 19th century for the decarboxylation of carboxylic acid. The application of electrochemistry in organic synthesis helps to scale up the manufacturing of organic products.<sup>[28,29]</sup> Due to the rapid, cost-effective, environmentally benign, and extensive synthetic application electrochemical method of C–H bond functionalization is considered a very effective technique among other traditional methods.<sup>[7]</sup>

Excellent heat and mass transfer, environmentally benign, and high productivity are some reasons why continuous flow electrochemical methods overcome the disadvantages of batch techniques and have been increasingly used as effective tools to boost the rate of chemical reactions.<sup>[20]</sup> Because of the several advantages of flow electro-organic synthesis such as due to small inter-electrodes distance small or no amount of electrolyte is consumed, continuous and safer reactions set-up, and the high surface-to-volume ratio of flow electrochemical reactor to catalyze the reaction, researchers are keen on developing the flow technique for C–H bond functionalization in organic synthesis. The implementation of the flow technique increases the rate and yield of chemical reactions.<sup>[2,7,30,31]</sup> The combination of flow technology and

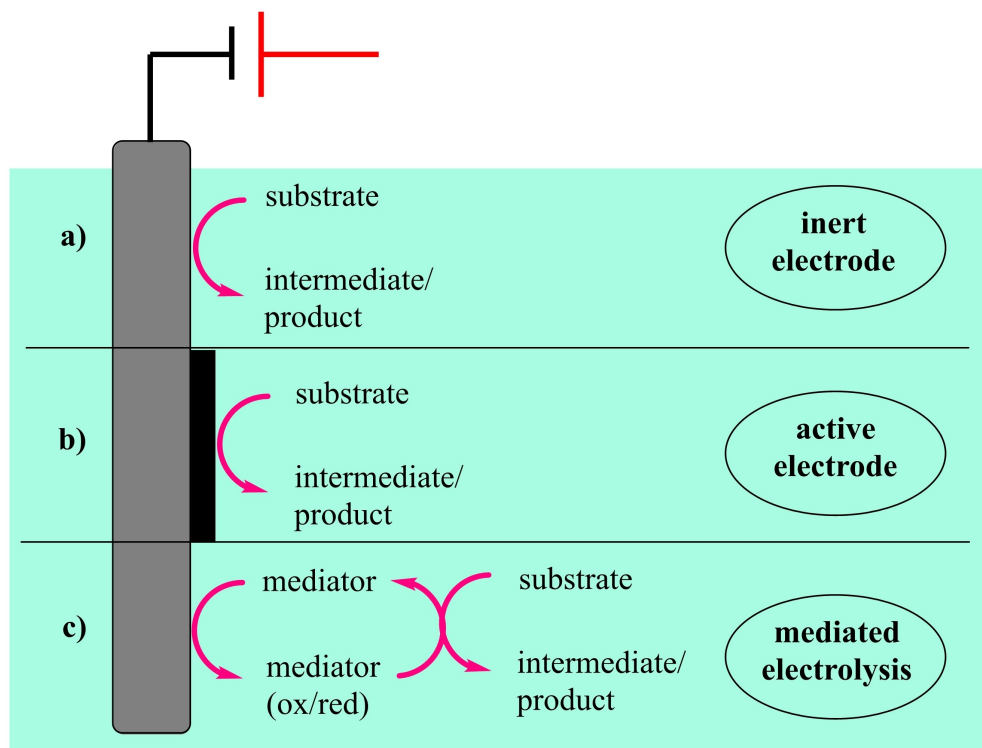


**Figure 1.** Different operation modes of electrodes in electro synthetic applications.<sup>[25]</sup>

electrochemistry provides very effective applications of electrochemistry. The development of microreactors enhanced the performance of the electrochemical flow reactions.<sup>[30]</sup> A thin layer flow cell microreactor can be constructed by separating thin electrodes by an adhesive non-conductive tape, with a very thin channel on it for movement of electrolyte solution. Microreactor is a reactor device with a microchannel on it about micrometer scale. Yoshida et al showed a microreactor with a PTFE membrane about 75  $\mu\text{m}$  thick and 3  $\mu\text{m}$  pore size.<sup>[32]</sup> Electrochemical flow cells are becoming increasingly popular over conventional batch electrochemistry. Flow electrochemistry helps to synthesize the complex organic compound by automated flow configuration. This method of the flow technique offers safety and economic benefits by reducing the need for the purification process. There is no question on more advantages of the flow electrochemistry over conventional techniques, commercialization of the flow electrochemistry is hindered by some challenges.<sup>[33]</sup>

It is well known that photoelectrochemical cells effectively transform sunlight into chemical fuel energy. Photoelectrochemical cells (PEC) were first reported in the early 1980's.<sup>[34]</sup> Researchers are nowadays more attracted to the study and development of photoelectrochemical cells, due to their endless, inexpensive, environmentally friendly, and endless renewable sunlight source.<sup>[35]</sup> The strong oxidizing power of photoanode and reducing the power of metal cathode of the PEC, make these cells applicable in different organic reactions. Comparatively inert C–H bonds of alkane can be functionalized using PEC, this cell is also commonly used for oxidation and coupling reactions.<sup>[36]</sup> Besides many advantages, there are some difficulties in using photoelectrochemical cells such as complex setup, no uniform standard for equipment, difficulty in reaction scale-up etc.<sup>[36]</sup>

## 1.1. Advantages of Flow Electrochemical Reactions

Flow electrosynthesis *via* microreactor is an environmentally friendly and green synthetic route for organic synthesis. Due to the microchannel and parallel large electrodes in the microreactor chamber, it increases activation process and reaction productivity. The main characteristics of the microreactor chambers are listed below.<sup>[37–41]</sup>

### 1.1.1. Temperature Control

The high surface-to-volume ratio of the microchannel allows rapid heat transfer, due to which the microreactor cools rapidly. The temperature controlling mechanism of the microreactor helps to conduct the reaction that requires high temperature.<sup>[42]</sup>

### 1.1.2. Safe reacting Mechanism for Hazardous Reagent

The invention of the electro-flow-based microreactor promotes environment-friendly organic synthesis. Unlike batch electrolysis, a small quantity of the reactant is required due to the micro-sized reacting channel. Hazardous and explosive chemical reactions can also be carried out in the electrochemical microreactor.<sup>[33]</sup>

### 1.1.3. High Temperature and Pressure Tolerance

Due to the fast heat transfer properties of the microreactor and small micro space in the channel, an electrochemical microreactor is advantageous for those reactions that require high temperature and pressure.<sup>[43]</sup>

### 1.1.4. Short Reaction Time

Minimum reaction mixing time between the reactants increases the rate of reaction. In a microreactor time required to diffuse the reactant is proportional to the square of the path length, therefore shortening of the path length speeds up the rate of reaction.<sup>[44]</sup>

### 1.1.5. Mass Transfer Between Phases

Due to the high surface-to-volume ratio of the microchannel, phase boundary reactions between gas/liquid, liquid/liquid, liquid/solid are more efficient.<sup>[42]</sup>

### 1.1.6. Sufficient Residence Time

Reactant molecules get sufficient time inside the microreactor channel to combine to give products. Due to the long microchannel reactant molecules can be converted into the product so the productivity of the reaction increases.<sup>[45]</sup>

## 1.2. C–C Bond Formation

Over the past decades, visible light photocatalysis has made possible the so-called inaccessible redox-neutral reactions that proceed via single electron transfer (SET) mechanism,<sup>[46,47]</sup> But this approach requires photocatalysts which have limitations like the significant tuning of redox potentials, high cost of the photocatalyst,<sup>[48]</sup> and difficulty in its removal during purification step,<sup>[49,50]</sup> Recently, Mo et al.<sup>[51]</sup> proposed microfluidic redox-neutral electrochemistry ( $\mu\text{RN-eChem}$ ) which applies to single-electron transfer (SET) redox-neutral chemistries. In conventional electrochemical systems, the larger electrode separation permits radical decomposition during their migration. But, in a microfluidic redox-neutral system, the inter-electrode gap is very thin and rapid radical transport occurs via

diffusion. Therefore, radical decomposition could be prevented so that cross-coupling product is formed selectively.<sup>[51]</sup> Mo et al.<sup>[51]</sup> designed a  $\mu$ RN-eChem flow cell with variable interelectrode separation (25 to 500  $\mu$ m). Two different glassy carbon (GC) plates were used to prepare electrodes. Thin fluorinated ethylene propylene (FEP) film was sandwiched in between the GC electrodes creating a thin-gap channel. The interelectrode distance was controlled by the thickness of the FEP spacer. The GC plates and FEP spacer were compressed in between two aluminum plates to ensure the sealing of the flow cell. An exploded view of the cell is shown in Figure 2.

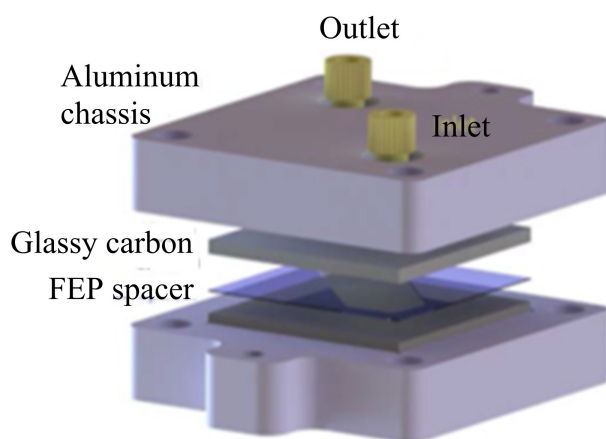


Figure 2. Exploded-view CAD drawing of the  $\mu$ RN-eChem flow cell.<sup>[51]</sup>

The basic conceptual framework of  $\mu$ RN-eChem designed by Mo et al.<sup>[51]</sup> for the cross-coupling reaction of persistent and transient radicals is illustrated in Figure 3.

To test the performance of the  $\mu$ RN-eChem system, Mo et al.<sup>[51]</sup> selected carboxylic acid as a precursor (decarboxylative Kolbe electrolysis) for an anodic transient alkyl radical whereas electron deficient aryl nitriles was selected as a precursor for cathodic persistent radical. On cathode, an electron deficient aryl nitrile **2** undergoes a SET event to form a persistent radical anion **4** (Scheme 1). At the same time, on the anode, alkyl carboxylic acid **1** is deprotonated in the presence of a Bronsted base to give carboxylate anion. The carboxylate anion then undergoes SET oxidation with subsequent loss of  $\text{CO}_2$  to form a transient alkyl radical **3** (Scheme 1). Finally, radical cross-coupling leads to the formation of the product **5** (Scheme 1).<sup>[51]</sup> From this experiment, Mo et al.<sup>[51]</sup> reported that the yields of cross-coupling products were reduced with increasing interelectrode distance. Moreover, they reported improved selectivity and scale-up of the  $\mu$ RN-eChem system over conventional electrochemical setup. The excellent conductivity in the microfluidic channel also omits the need for additional supporting electrolyte.<sup>[51]</sup>

Note: R-COOH, carboxylic acid (where R is the alkyl group);  $\text{R}^\bullet$ , alkyl radical; EWG, electron-withdrawing group

Radical cross-coupling is an almost diffusion-controlled phenomenon. Therefore, selective cross-coupling of radicals is a challenging task. However, if the rate of formation of persistent radical and transient radical is the same and their

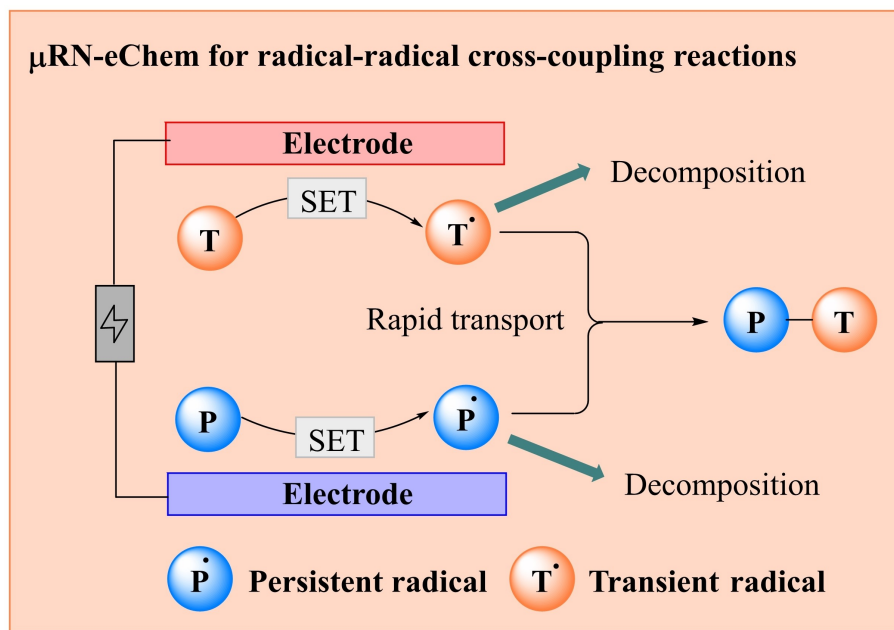
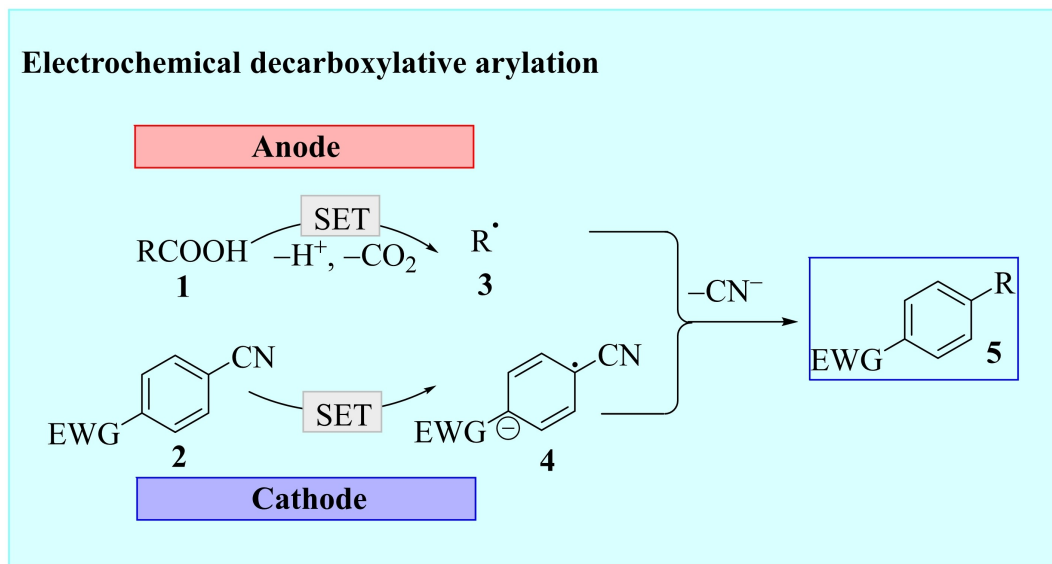


Figure 3. Concept of  $\mu$ RN-eChem for the cross-coupling reaction of persistent and transient radicals. ( $t$ =time,  $d$ =interelectrode distance,  $D$ =molecular diffusivity).<sup>[51]</sup>



**Scheme 1.** Mechanism of Redox-neutral Electrochemical Cross-coupling Reaction of Carboxylic Acids and Electron Deficient Aryl Nitriles.<sup>[51]</sup>

lifetime is different, selective cross-coupling becomes dominant. This kinetic phenomenon of selective cross-coupling is called persistent radical effect (PRE).<sup>[52]</sup>

Momeni and Nematollahi<sup>[53]</sup> designed a parallel plate flow reactor for the electrochemical synthesis of inherently active compound, quinone sulfonimide (QSI) **10** by oxidation of 4-aminophenyl ether (APE) **6** in the presence of arylsulfonic acids (ASAs) **8**. *p*-quinone-imine (QI) **7** was generated electronically and it further reacted with ASA to form QSI (Scheme 2). In this way, QSIs were synthesized in a short time with excellent yields and purity without using supporting electrolyte.<sup>[53]</sup> The cell design includes a flow cell with eight rectangular parallel plates. A carbon plate (with a thickness of 6.0 mm) was used as an anode whereas stainless steel plate (with a thickness of 2.0 mm) was used as a cathode. At the back of the carbon electrode, a copper plate (1.0 mm thickness) was placed to improve the potential distribution. The thickness of the spacer controls the interelectrode distance (Figure 4).<sup>[53]</sup>

Note: 1. Top iron plate. 2. Insulating plexiglass plate. 3. Stainless steel cathode plate. 4. PTFE spacer with flow channels. 5. Carbon anode plate. 6. Cu plate. 7. Plexiglass plate. 8. Bottom iron plate. 9. Peripheral bolt. 10. Inlet. 11. Outlet.

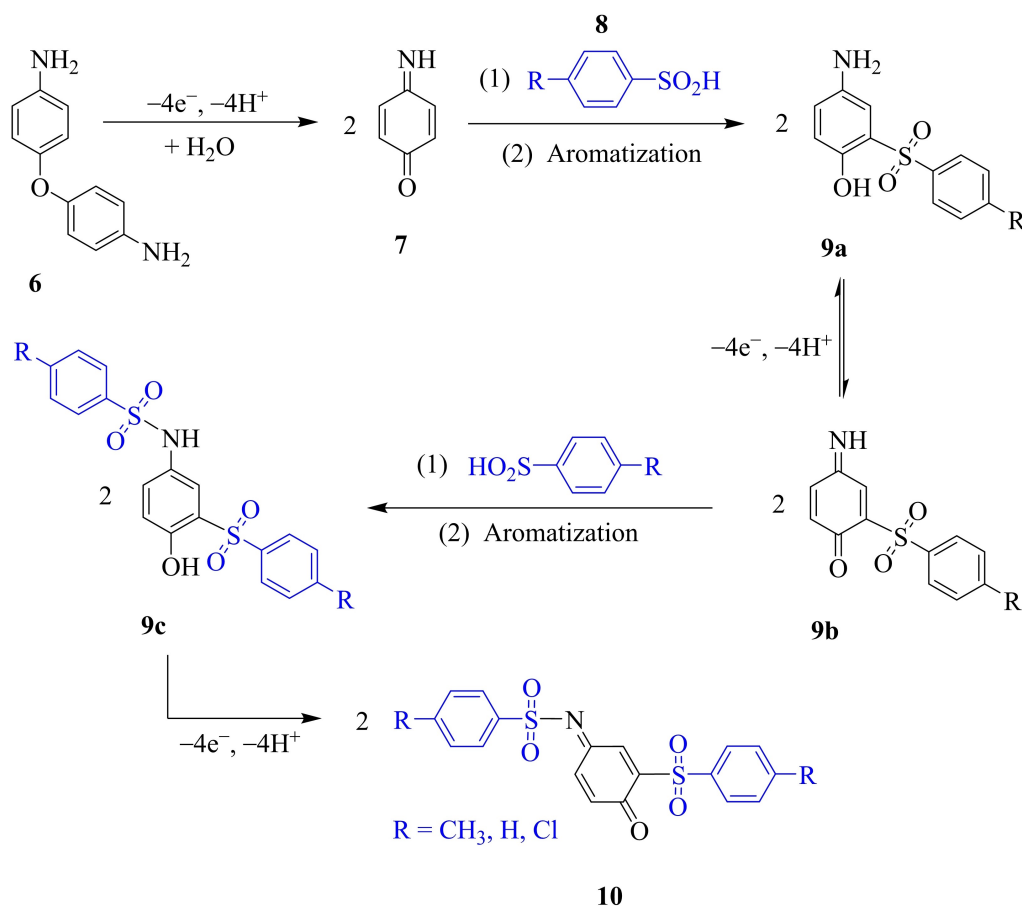
Most recently, Momeni and Nematollahi<sup>[54]</sup> synthesized different biologically important pyrimidine derivatives by using electrochemical batch reactor and electrochemical flow reactor. Different catechols (**11a-c**) were converted into their pyrimidine derivatives (**13-15**) in the presence of barbituric acid derivatives (**12**) with excellent yield (Scheme 3). Some of the products were spiro compounds.<sup>[54]</sup> The setup for a flow cell

includes a working electrode of rectangular graphite plate (200 × 100 × 6 mm) and a counter electrode of stainless-steel plate (200 × 100 × 1 mm), channel length was 190.0 mm with 6.0 mm width and interelectrode gap of 1.0 mm. Likewise, in batch synthesis, carbon rod anode and stainless-steel cathode were used in 0.15 M sodium acetate solution.<sup>[54]</sup>

### 1.2.1. Flow-Metallaelectro-Catalyzed C–H Activation

C–H bonds in organic compounds can be functionalized oxidatively by using oxidants such as copper(II) and silver(I) salts.<sup>[55]</sup> As compared to the oxidation potentials of common functional groups and organic solvents, the oxidation potentials of the C–H bond are higher. This renders a serious challenge in the site-selective anodic oxidation of C–H bonds.<sup>[56]</sup> Therefore, to avoid the unwanted oxidation of other functional groups and solvents, a mediator (redox catalyst) assisted indirect electrolysis is used in which initially electron transfer occurs between electrode and mediator and then between mediator to reactants.<sup>[57]</sup> Transition metal catalysts are considered as one of the best candidates for mediators because simply a ligand modification can access the tuning of redox potentials of these complexes so that over potentials can be prevented. Therefore, as an alternative strategy, a combination of electrochemistry and transition metal catalysis can afford a synergistic effect for site-selective C–H functionalization.<sup>[58]</sup>

The major challenges of the flow-metallaelectrocatalytic C–H activation are harsh reaction conditions, effective mass and electron transfer, and undesired cathodic reduction of the catalyst.<sup>[55]</sup> Kong et al.,<sup>[55]</sup> for the first time, devised a flow-



**Scheme 2.** Electrochemical Oxidation Pathway of APE in the presence of ASA.<sup>[53]</sup>

rhodaelectro-catalyzed system for the annulation of aryl imidate **16** and unsymmetrical alkyne **17** (Scheme 4). The cell design includes porous graphite felt (GF) anode and a nickel plate (Ni) cathode with a thin meshed PTFE plate as a turbulence promoter between the anode and cathode. A peristaltic pump was used to pump the solution from the external reservoir to the flow reactor (Figure 5).<sup>[55]</sup> Further optimization of the cell leads to 83% yield of the product **21** by annulation of alkyne **20** with imidate **19** (Scheme 5). For this synthesis, methanol was used as a solvent, 2.5 mol%  $[\text{RhCp}^*\text{Cl}_2]_2$  as a catalyst, and sodium pivalate (NaOPiv) and pivalic acid (HOPiv) as additives.<sup>[55]</sup>

The versatility of the approach was further tested with different imidates substrates which were successfully converted into annulated products. For instance, the annulated products **24a**, **24b**, **24c**, **24d–e**, and **24f** were obtained from the corresponding imidates: sterically hindered isopropyl benzimidate, imidates with electron-releasing groups, imidates with electron withdrawing groups, heterocyclic imidates, and cyclohexene imidate, respectively (Scheme 6). The approach was

also applicable to intramolecular annulation of the species **25** to give azo-tetracycle **26** (Scheme 7). A high level of functional group tolerance, regioselectivity, and easy scale-up was reported as salient features of the approach.<sup>[55]</sup>

### 1.2.2. C–C Bond Formation Using Flow-Metallalectro-Catalyzed System

Li et al.<sup>[59]</sup> designed a method for C–C bond formation which uses N-hydroxyphthalimide esters (NHP esters) as a radical precursor. They reported continuous flow Ni-catalyzed electrochemical decarboxylative C–C coupling of NPH esters **27** with aryl halides **28** (Scheme 8). The reaction was performed in a divided electrochemical flow-cell using tertiary amine as a reductant. Electrochemically generated highly reactive radicals were incorporated into Ni-catalyzed  $\text{Csp}^3\text{–Csp}^2$  coupling manifold to synthesize structurally diverse molecules.<sup>[59]</sup>

The cell design includes a C-flow cell with reticulated vitreous carbon (RVC) foam attached to the anode and cathode graphite plates. The RVC foam helps to increase the

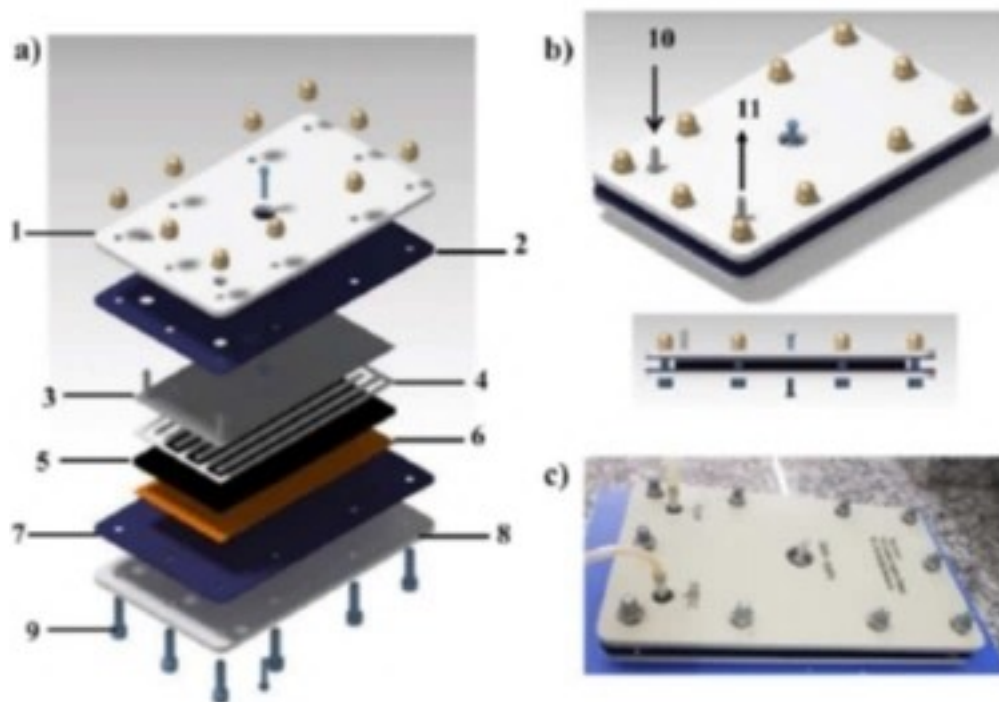
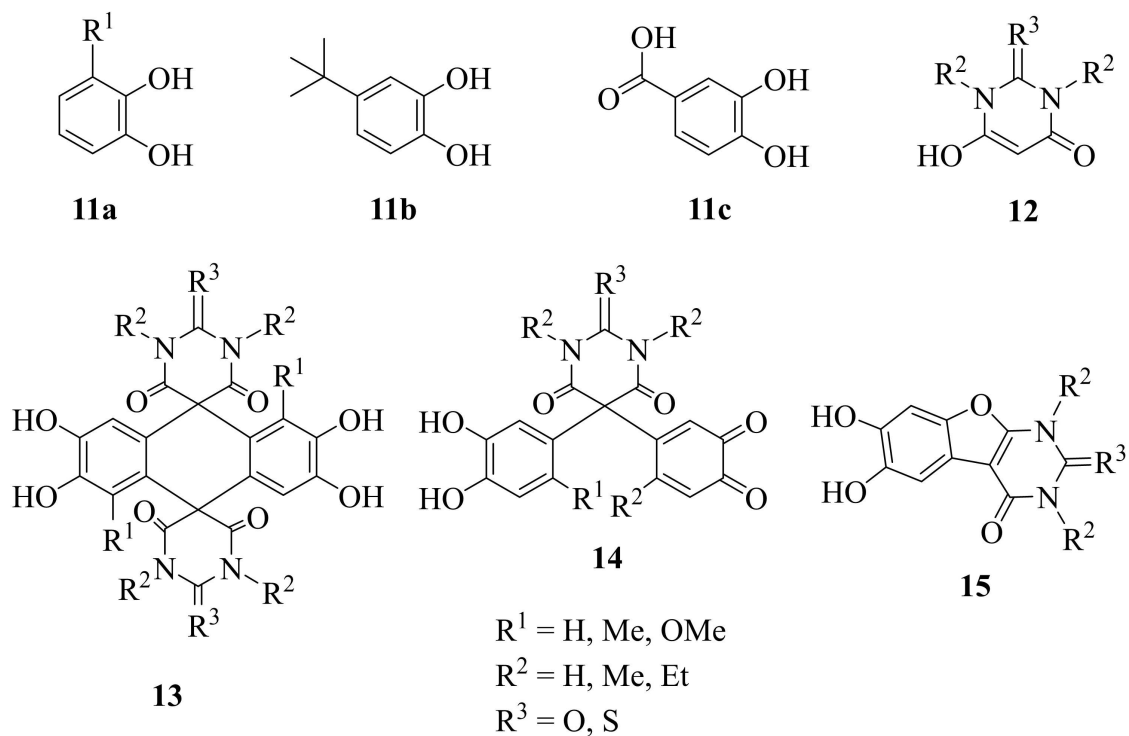
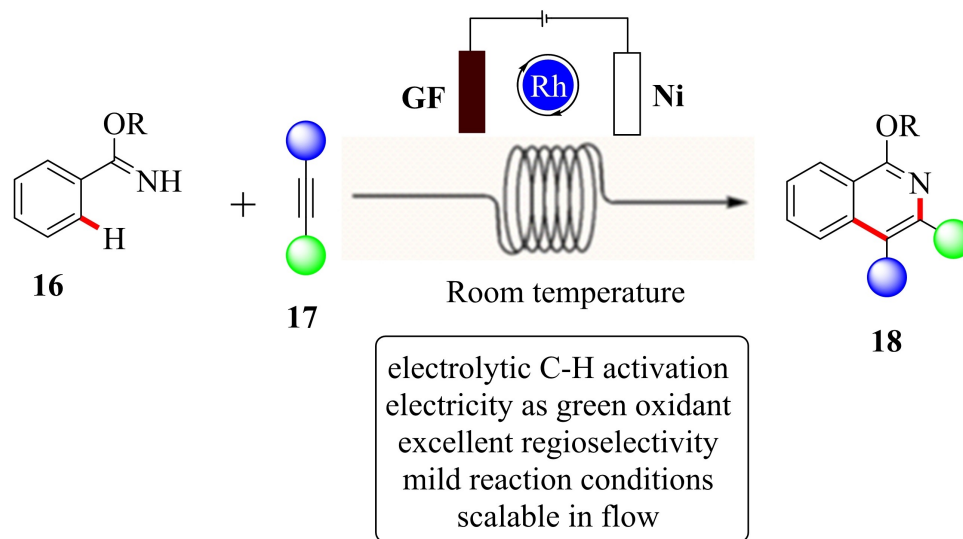


**Figure 4.** Schematic of designed and constructed flow electrolysis cell. (a) Exploded view of the cell. (b) Assembled and *side* view of the cell. (c) Photograph of reactor.<sup>[53]</sup>



**Scheme 3.** The structures of Catechol (11a-c), barbituric acid (12) derivatives, and synthesized products (13-15).<sup>[54]</sup>



**Scheme 4.** Flow-rhodalectro-catalysed C-H Annulation. GF: graphite felt.<sup>[55]</sup>

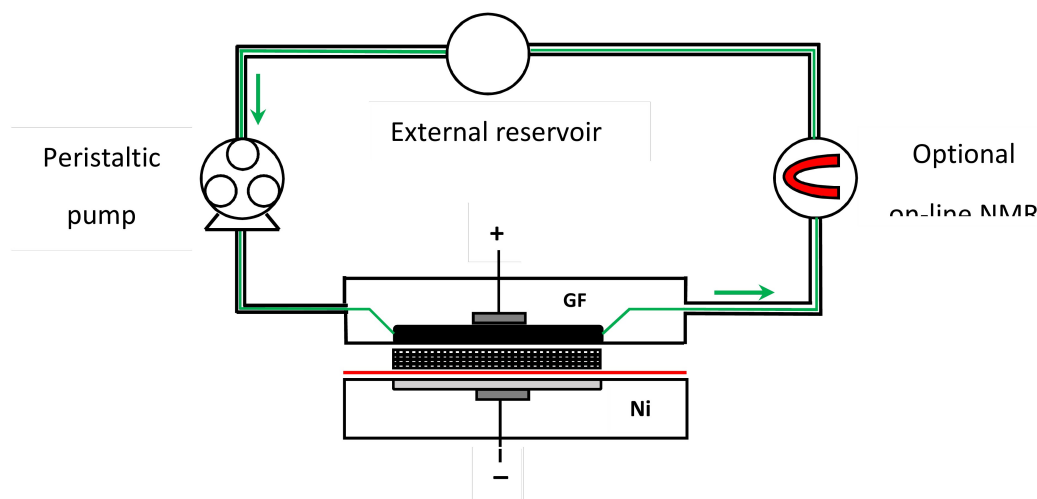


**Figure 5.** Schematic representation of the electrochemical flow reactor with rubber gasket (red) and turbulence promoter (meshed).<sup>[55]</sup>

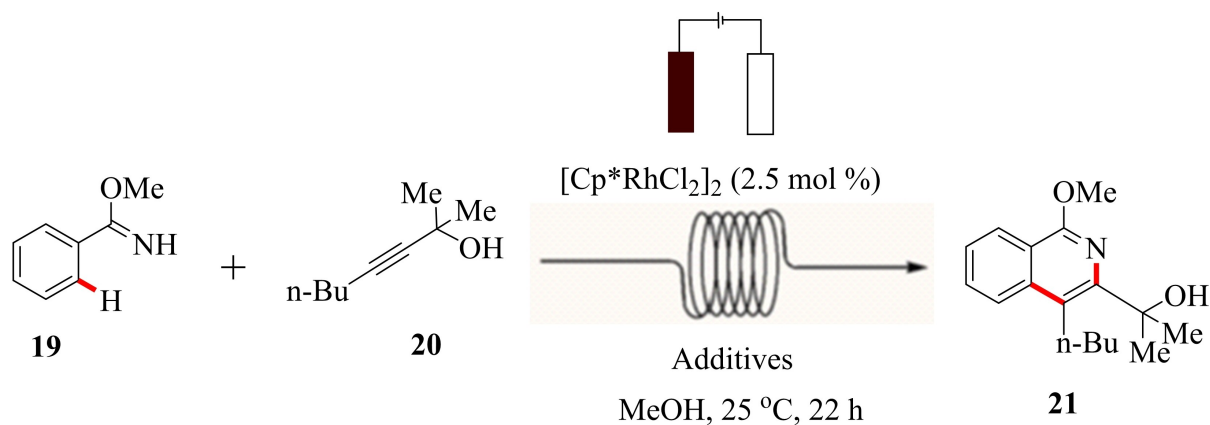
surface area of the electrodes. Anodic and cathodic streams were delivered into the electrochemical cell by using a Harvard syringe pump. The two streams were separated by a Nafion membrane which allows the cross-membrane flow of ions but not neutral molecules (Figure 6, Figure 7).<sup>[59]</sup>

The proposed mechanism of the reaction is that, at the cathode, the redox-active NHP ester **30** is reduced and decarboxylative fragmentation results in the formation of  $C_{sp^3}$  alkyl radical **31**. At anode oxidative addition of aryl halide on Ni-catalyst forms homogeneous either Ni(0) or Ni(II) species. Then, the alkyl radical is intercepted by the Ni(0) or Ni(II) species to form Ni(III) species **32**. Finally, reductive elimination leads to the formation of  $C_{sp^3}$ - $C_{sp^2}$  coupling product

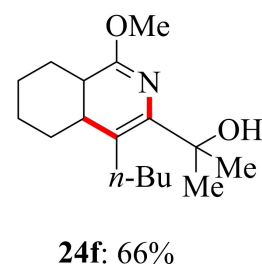
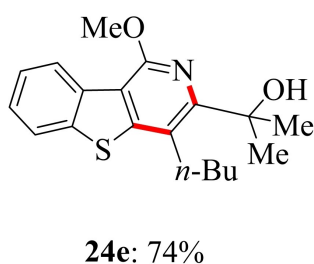
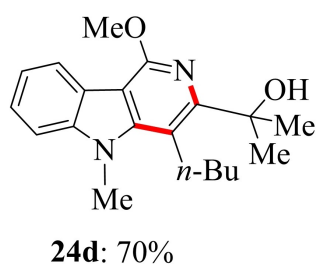
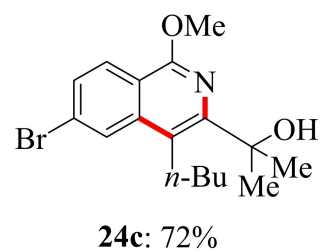
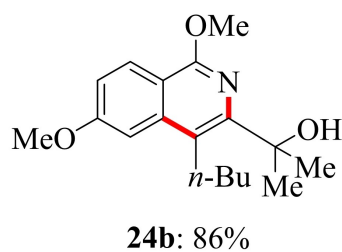
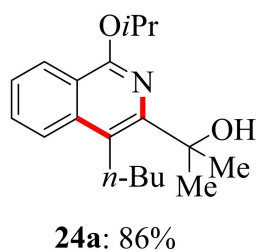
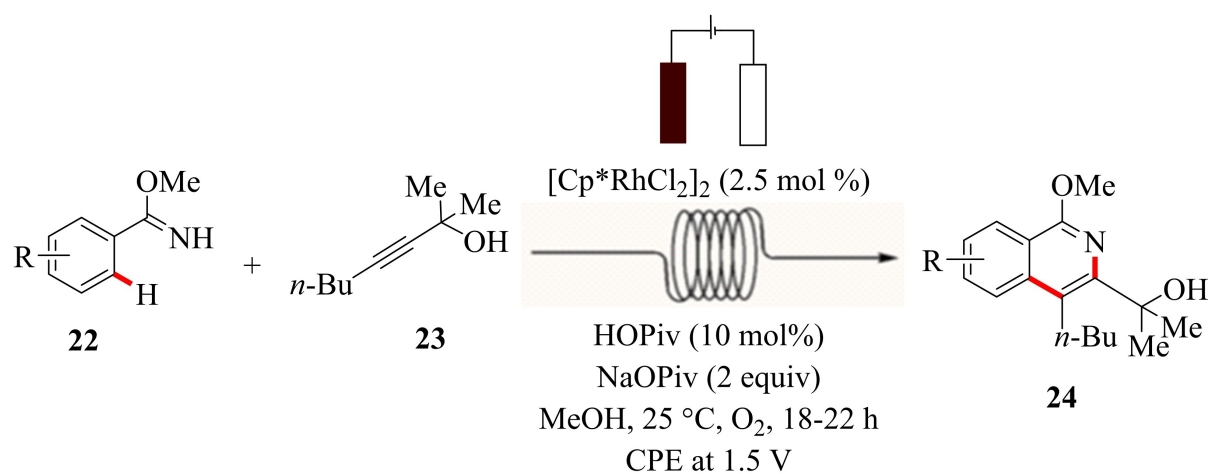
**33** and Ni(I) species (Scheme 9). At the cathode, the Ni(I) would be reduced to Ni(0) thereby halting the catalytic cycle. Therefore, electron-rich tertiary amines are used as a sacrificial reductant that supplies electrons to the electrochemical system after their anodic oxidation.<sup>[59]</sup>

### 1.2.3. Electrochemical Microflow System (Cation Flow Method)

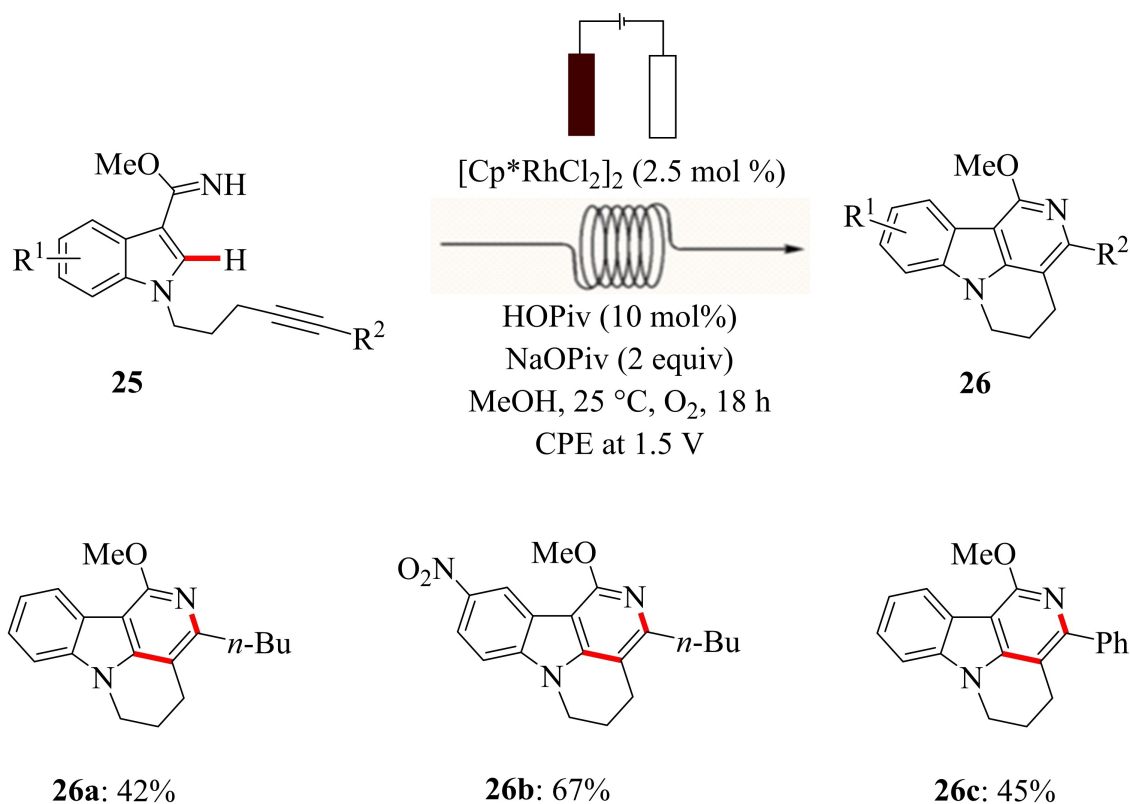
Suga et al.<sup>[60,61]</sup> designed a cation flow method that involves the continuous generation of a carbocation in the absence of nucleophiles by low-temperature electrolysis. The carbocation so formed were then reacted with carbon nucleophile in the



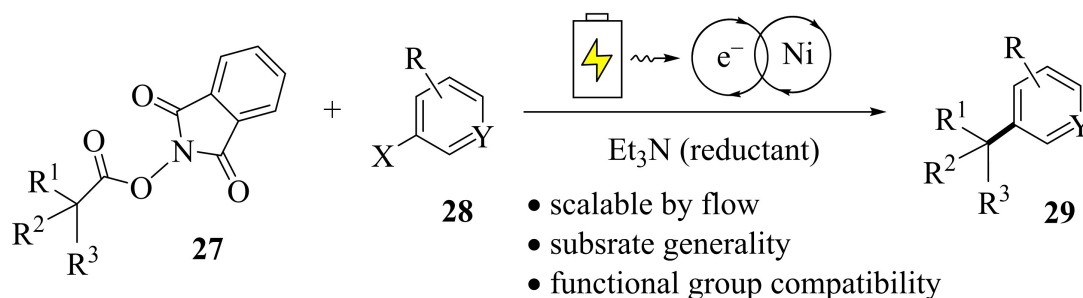
**Scheme 5.** Flow-rhodaelectro-catalysed C-H Annulation of Alkyne with Imidate.<sup>[55]</sup>



**Scheme 6.** Flow-Rhodaelectro-Catalyzed C-H Activation with Imidates.<sup>[55]</sup>



**Scheme 7.** Intramolecular Flow-Rhodiaelectro-Catalyzed C–H Activation.<sup>[55]</sup>



**Scheme 8.** Ni-catalyzed Continuous Flow Electrochemical Decarboxylative Coupling of N-Hydroxyphthalimide Esters with Aryl Halide.<sup>[59]</sup>

microflow system to achieve direct oxidative C–C bond formation. The reactor was made of a diflone and stainless-steel body. The cell contains two compartments separated by a polytetrafluoroethylene (PTFE) membrane (Figure 8). Dry ice baths were used to lower the temperature of the system which avoided the decomposition of carbocations. Carbocations were generated at the anode (made of carbon felt) whereas nucleophiles were generated at the cathode (made of Pt wire) and they were directly reacted to form C–C bond in the final product (Figure 9).<sup>[60,61]</sup>

To test the effectiveness of the cation flow method, methyl pyrrolidinecarboxylate **18** (a carbamate) was used as a carbocation precursor and allyltrimethylsilane was used as a nucleophile (Scheme 6). Solution of methyl pyrrolidinecarboxylate in DCM with  $\text{Bu}_4\text{NBF}_4$  as supporting electrolyte was pumped to the anodic chamber and solution of the supporting electrolyte and trifluoromethanesulphonic acid (TfOH) was injected into the cathodic chamber (with a platinum wire cathode) as a proton source. Then, low-temperature electrolysis of **34** (Scheme 10) forms carbocation intermediate which is immediately transferred to a vessel in which it reacts with a

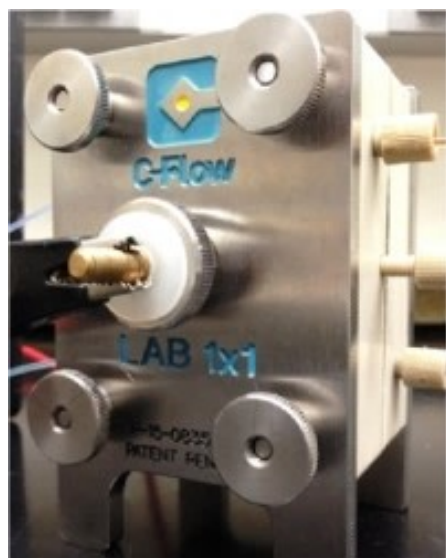


**Figure 6.** Continuous-flow electrochemical cell designed by Li et al. for Ni-catalysed decarboxylative arylation.<sup>[59]</sup>

nucleophile (allyltrimethylsilane) to form the final coupling C–C formation product **35** (Scheme 10).<sup>[60,61]</sup>

#### 1.2.4. C–C Bond Formation Using Electrochemical Paired Microflow System

Since only the anodic oxidation is utilized in the cation flow method, the cathodic reaction is sacrificial and H<sub>2</sub> is generated from H<sup>+</sup> and has low efficiency.<sup>[61]</sup> Therefore, Suga et al.<sup>[61]</sup> extended the cation flow method to a more effective electrochemical paired microflow system in which both the anodic oxidation and cathodic reduction play a role in the product formation. The two-compartment reactor divided by a

diaphragm of PTFE membrane was designed. Each compartment has a channel (width  $W$  1.5 mm × depth  $D$  4 mm × length  $L$  57 mm), which is filled with carbon felt electrode made of carbon fibers ( $\phi = 10 \mu\text{m}$ ) (Figure 10, Figure 11).<sup>[61]</sup> A carbocation is generated at the anode whereas a nucleophile is generated at the cathode. In paired electrolysis, at the anode, silyl-substituted carbamate **36** was oxidized to generate an *N*-acyliminium ion and at the cathode cinnamyl chloride **37** was reduced to cinnamyltrimethylsilane **38** in the presence of chlorotrimethylsilane. Finally, compounds **37** and **38** undergo cross-coupling to yield compound **39** (Scheme 11).

Later on, Suga et al.<sup>[62]</sup> designed an integrated synthesis to combine multiple components in a single step instead of a conventional step-by-step synthesis. They performed experiments based on time integration and space integration and reported that space integration using flow microreactor systems is more effective than time integration.<sup>[62]</sup> In the time integration experiment, carbocation intermediate *N*-acyliminium ion **41** was generated by the cation pool method which was stirred with an electron-rich optically active olefin *2-t*-butyl-3-methoxycarbonyloxazole **40** for 10s at a  $-78^\circ\text{C}$  to generate a new cation pool **42**. During this, cation **41** was added regioselectively to the carbon-bearing oxygen in **40**. The newly formed cationic species **42** was reacted with allyltrimethylsilane (carbon nucleophile precursor) to give C–C coupling product **43** as a single diastereomer in 54% yield. Hydrolysis of the compound **43** in the presence of TfOH as catalyst formed **44** with 81% yield (Scheme 12).<sup>[62]</sup>

Likewise, space integration was examined by using a microflow system. Suga et al.<sup>[62]</sup> designed a microflow reactor system with two micro-mixtures (**M1** and **M2**) and two microtube reactors (**R1** and **R2**). Compound **40** was mixed with cation **41** in **M1** to form cation **42**. Then, the cation **42** was reacted with allyltrimethylsilane in **M2** to give the product **43** (Scheme 13). The yield of the product was 79% which was

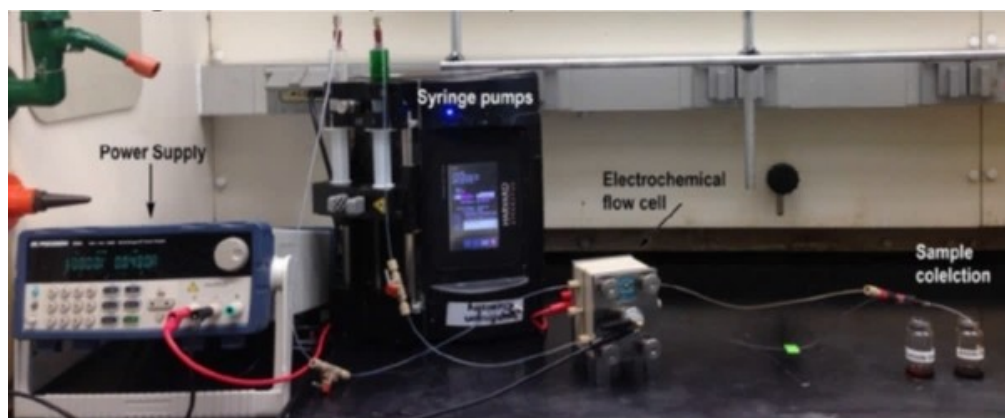
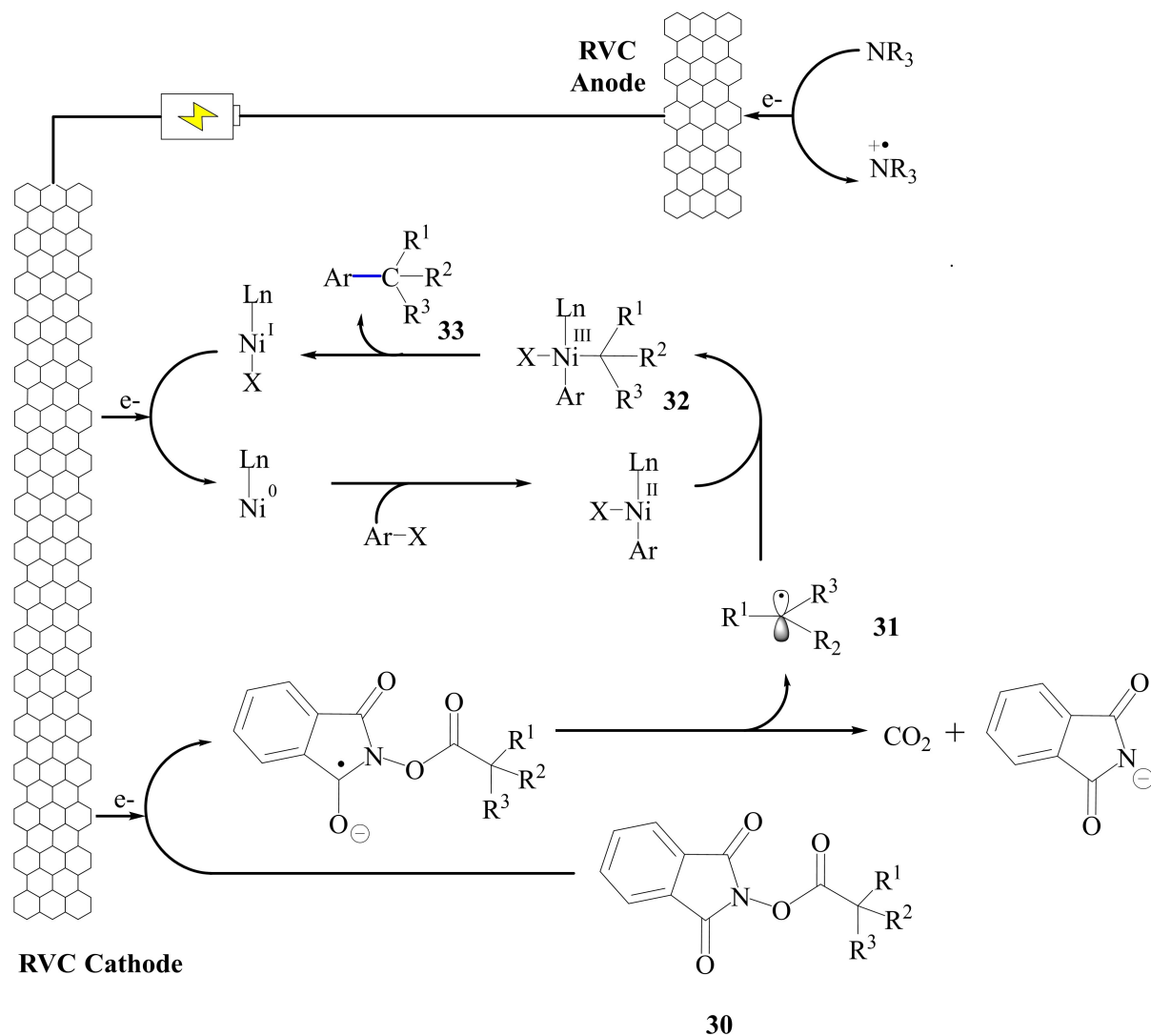


**Figure 7.** Overall setup for reaction performed in a continuous-flow mode.<sup>[59]</sup>



**Scheme 9.** Proposed Electrochemical-driven Nickel-catalysed Decarboxylative Arylation Unit Steps.<sup>[59]</sup>

significantly higher than that obtained with time integration. The reaction was carried out even at 0°C (much higher than in the time integration approach) and due to higher temperature conditions reaction was faster with better yield.<sup>[62]</sup>

Horii and co-workers<sup>[63]</sup> developed an electro synthetic system for anodic substitution reaction using a micro-flow reactor. They used a parallel laminar flow technique in which electrolytic solutions containing substrate and nucleophile were introduced via inlet **1** (anode side inlet) and inlet **2** (cathode side inlet), respectively (Figure 12). The channel of the microflow reactor is so small that the flow of the streams becomes parallel and laminar with a stable liquid-liquid interface. Carbocations generated at the anodic side rapidly diffuse to the bulk of the electrolytic solution and react with nucleophile at the cathodic side to form the product. Parallel

laminar flow of the carbocation and nucleophile streams in the reactor prevented the nucleophile from reaching the anode and hence unwanted oxidation of the nucleophile does not occur. The issues related to the stability of the carbocation were overcome by using carbocation stabilization ionic liquid and fast diffusion of the carbocation that is possible in the laminar flow technique.<sup>[63]</sup>

As a representative reaction, Horii and co-workers<sup>[63]</sup> performed anodic substitution of *N*-(methoxycarbonyl)pyrrolidine **45** with allyltrimethylsilane **46** to form the compound **47** (Scheme 14). They reported that the use of carbocation stabilizing solvent 2,2,2-trifluoroethanol (TFE) dramatically increased the yield of product **47**. The yield of **47** was further improved by using ionic liquid.

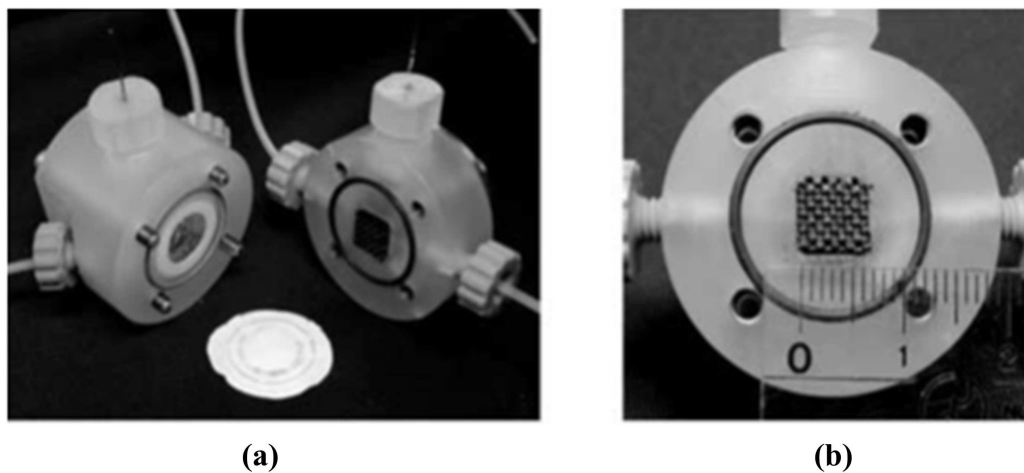


Figure 8. Electrochemical microflow reactor used for cation flow method. (a) outside (b) inside.<sup>[61]</sup>

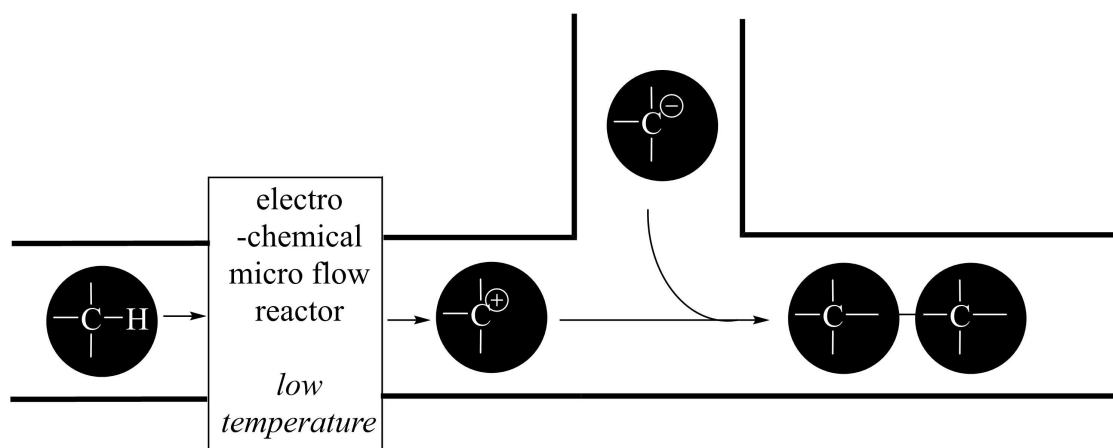


Figure 9. Electrochemical microflow system (cation flow method).<sup>[61]</sup>

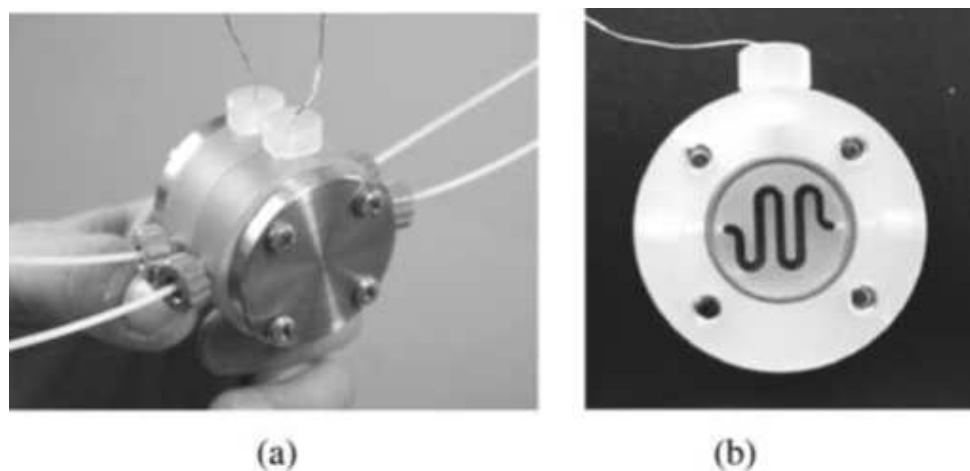
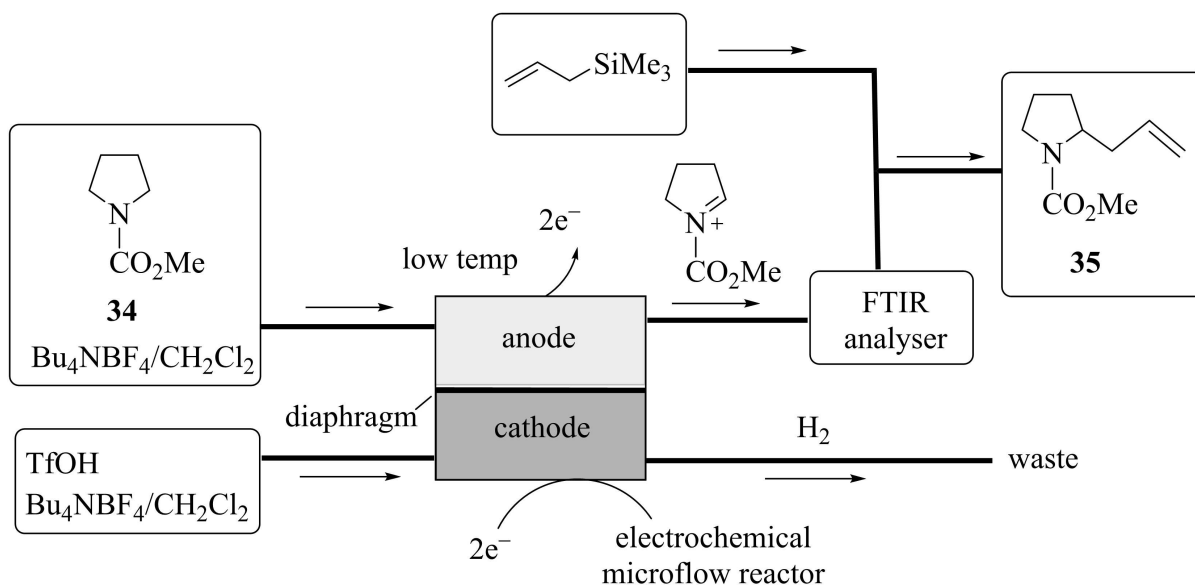
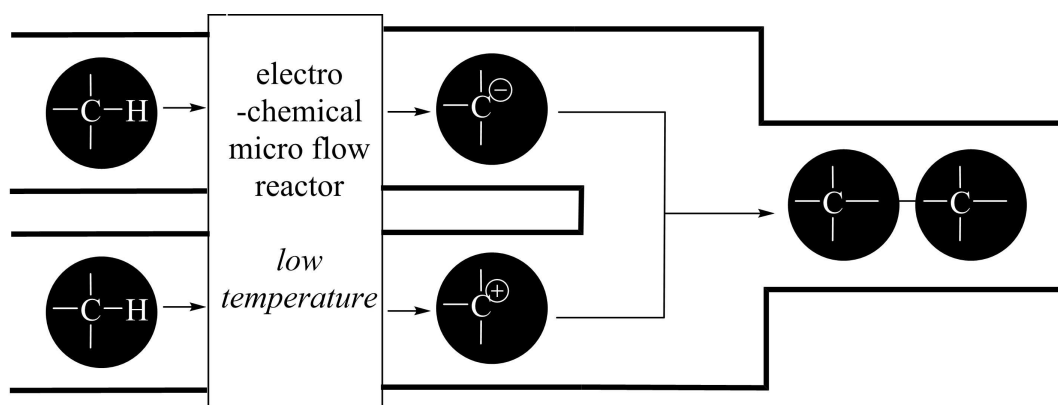


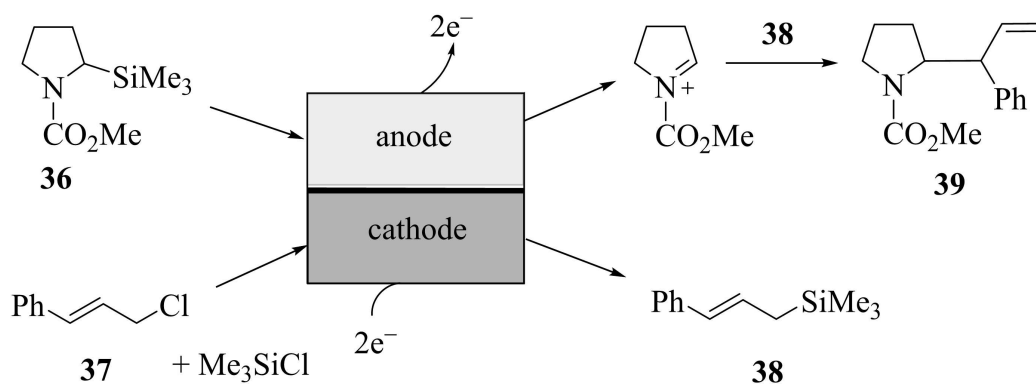
Figure 10. A microreactor composed of diflone and stainless-steel bodies designed for paired electrolysis: a) outside; b) inside.<sup>[61]</sup>



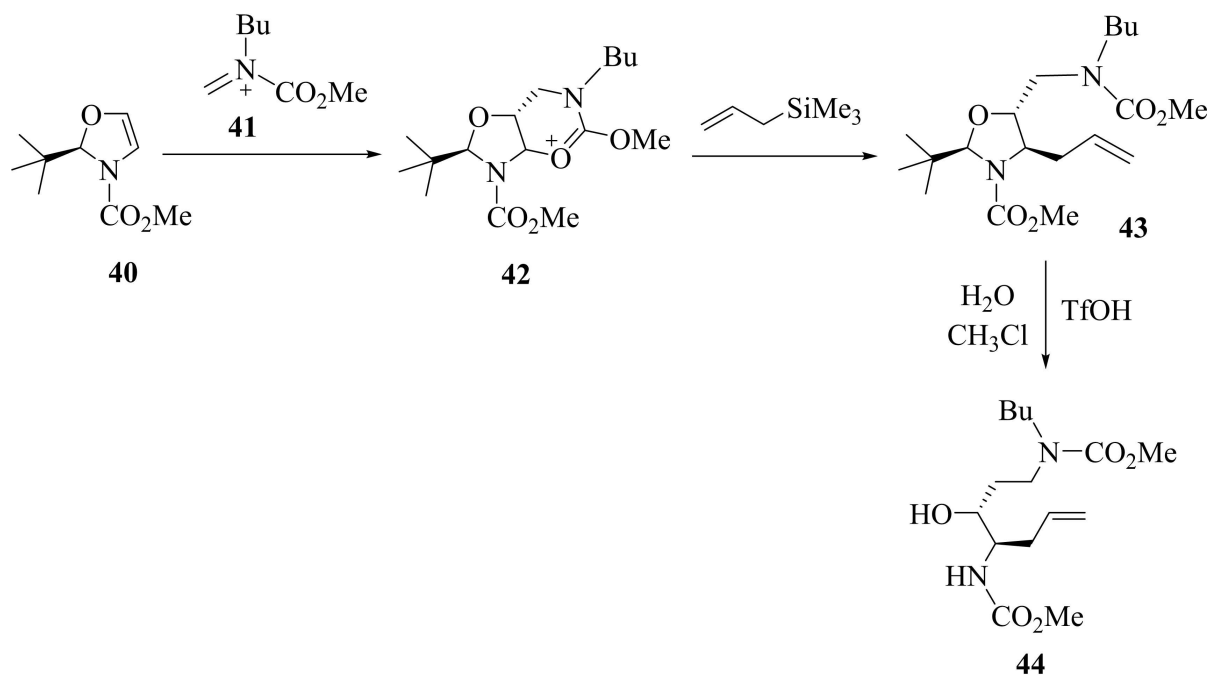
**Scheme 10.** Schematic Diagram of "Cation Flow" System for a Typical Reaction.<sup>[60,61]</sup>



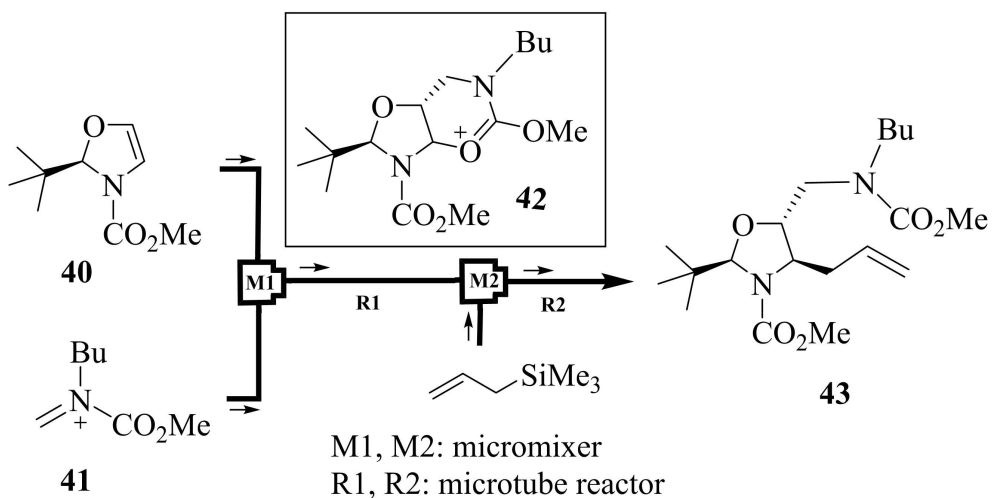
**Figure 11.** Electrochemical paired microflow system.<sup>[61]</sup>



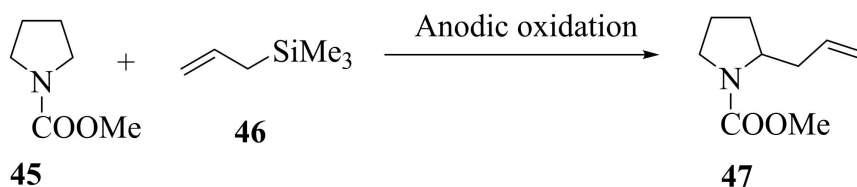
**Scheme 11.** Paired Electrolysis of 36 and 37 Using the Microflow System.<sup>[61]</sup>



**Scheme 12.** Cationic Three-component Coupling of Compound **40**, Cation pool of **41**, and Allyltrimethylsilane Based on Time Integration Followed by Hydrolysis.<sup>[62]</sup>



**Scheme 13.** Space Integration of Cationic Three Component Coupling.<sup>[62]</sup>



**Scheme 14.** Anodic Substitution Reaction of **45** with **46**.<sup>[63]</sup>

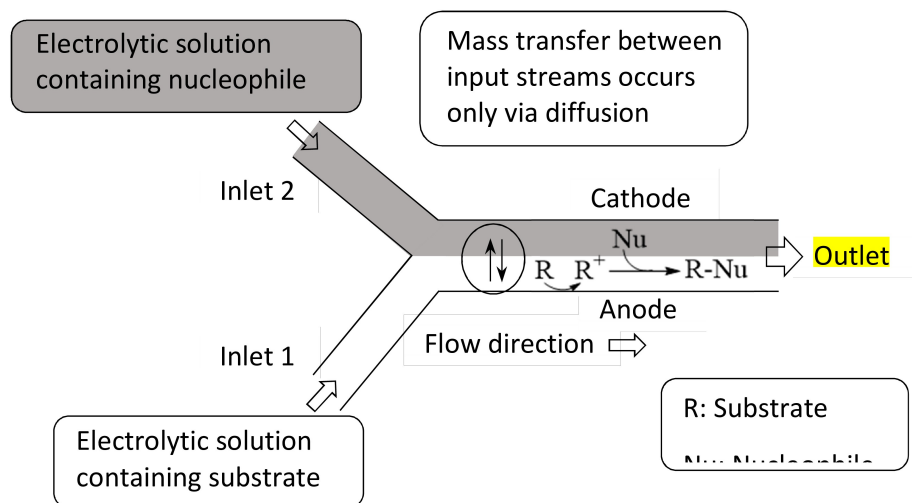
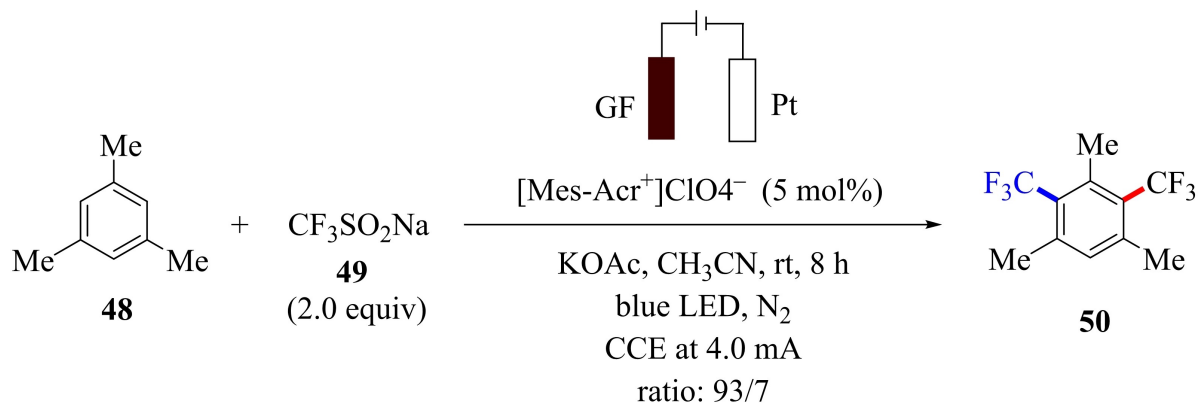


**Figure 12.** Schematic representation of parallel laminar flow in the micro-flow reactor. The illustrated model is an anodic substitution reaction in the reactor.<sup>[63]</sup>

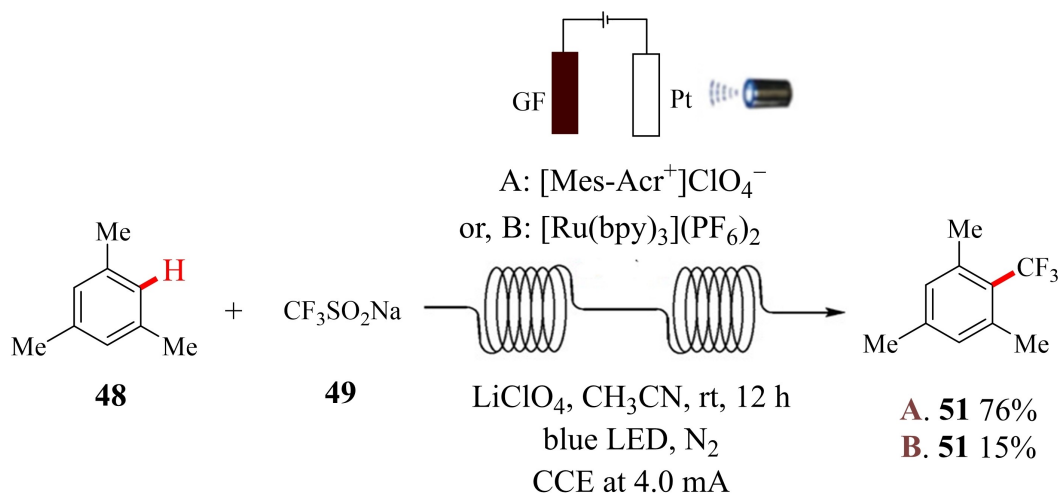
### 1.2.5. C–C Bond Formation Using Electro-Photochemistry

Recently, Qiu et al.,<sup>[64]</sup> for the first time, developed a sustainable electro-photochemical method for C–H trifluoromethylation of non-activated arenes through single electron transfer (SET) under mild reaction conditions. They performed electrophotochemical non-directed C–H trifluoromethylation of readily accessible mesitylene **48** with Langlois reagent **49** ( $\text{CF}_3\text{SONa}$ ) in an undivided batch cell with platinum plate cathode and graphite felt (GF) anode. In the preliminary reaction,  $[\text{Mes-Acr}^+]\text{ClO}_4^-$  was used as a photocatalyst, KOAc as a conductive additive, and  $\text{CH}_3\text{CN}$  as a solvent. The desired product **50** was obtained in 48% yield with mono to di-trifluoromethylated product ratio 93:7 (Scheme 15). However, after further examination, the process was optimized for a metal-free photocatalyst  $[\text{Mes-Acr}^+]\text{ClO}_4^-$  and ruthenium photocatalyst  $[\text{Ru}(\text{bpy})_3](\text{PF}_6)_2$  because the

best yield of the product **50** was reported with these reagents. With  $[\text{Mes-Acr}^+]\text{ClO}_4^-$  as a photocatalyst, the highest yield was obtained when  $\text{LiClO}_4$  was used as an additive in  $\text{CH}_3\text{CN}$  solvent (the yield was 85% with mono to di-trifluoromethylated product ratio 93:7), whereas with  $[\text{Ru}(\text{bpy})_3](\text{PF}_6)_2$  as a photocatalyst, the yield was 88% with 78:22 mono to di-trifluoromethylated product ratio.<sup>[64]</sup> The electrophotochemical C–H trifluoromethylation of mesitylene was also performed in an electro-flow cell with graphite and nickel as anode and cathode, respectively. With  $[\text{Mes-Acr}^+]\text{ClO}_4^-$ , the yield of the desired product **51** was 76%, whereas with  $[\text{Ru}(\text{bpy})_3](\text{PF}_6)_2$  that was only 15% (Scheme 16).<sup>[64]</sup>



**Scheme 15.** Preliminary Electrophotochemical C–H Trifluoromethylation.<sup>[64]</sup>



**Scheme 16.** Electrophotochemical C–H Trifluoromethylation in Electrochemical Flow Reactor.<sup>[64]</sup>

### 1.2.6. C–C Bond Formation Using Electrochemical Continuous Flow System

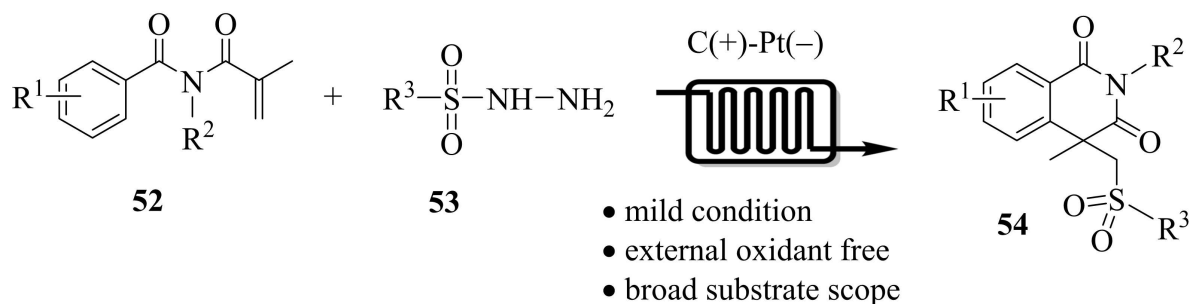
Recently, Xu et al.<sup>[65]</sup> developed an electrochemical continuous flow method for the synthesis of 4-(sulfonylmethyl)isoquinoline-1,3(2H,4H)-diones **54** via oxidative coupling of *N*-alkyl-methacryloyl benzamides **52** and sulfonylhydrazides **53** (Scheme 17). They synthesized varieties of sulfonylated products in moderate to excellent yields and reported excellent functional group compatibility of method.<sup>[65]</sup>

The electro-organic technique is a powerful, environment friendly, and effective approach to obtain symmetrical and nonsymmetrical biphenyls.<sup>[66]</sup> In this experiment, electrochemical synthesis of 3,3',5,5'-tetramethyl-2,2'-biphenol **56** (Scheme 18) has been studied by changing different parameters like current density, inter-electrodes gap, the concentration of starting materials, etc.<sup>[66]</sup> Current density were applied at a range between 2.4–45 mA/cm<sup>2</sup> however higher current density of 45–60 mA/cm<sup>2</sup> is found to be effective and also reduce the electrolysis time. The inter-electrodes gap was studied on 3 types 0.05 cm, 0.025 cm, 0.012 cm. An inter-electrodes gap of

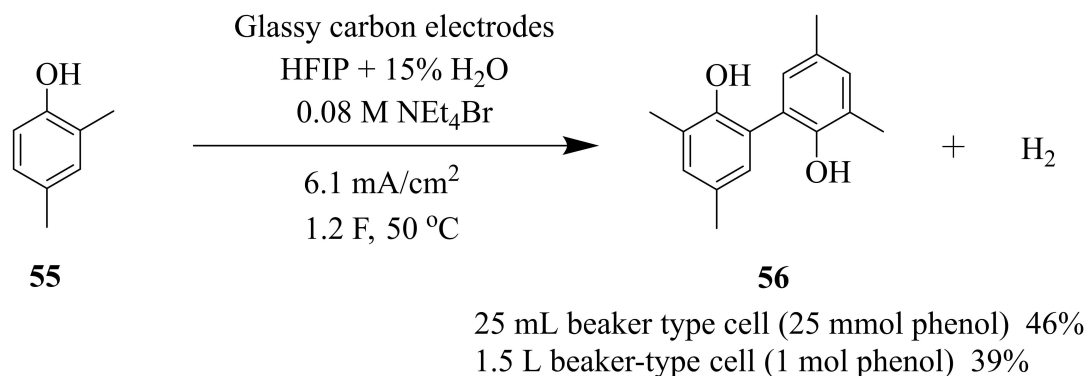
0.025 cm was found to be more effective among them. Another parameter concentration of the starting material had not shown any significant effect on 0.5 mol/L and 2.0 mol/L concentrations; however, the concentration of 2.0 mol/L is highly advantageous. By analyzing the different parameters, optimized conditions were fixed. Using the same cell geometry different sized electrochemical cells were used to achieve stepwise scale-up of products. For example 2×6 cm flow electrolysis cell (Figure 13), (4×12 cm flow electrolysis cell (Figure 14), and EUT pilot cell 2×6 cm electrolysis cell (Figure 15) were studied comparatively. Table 1 represents the comparative study of achieving scale-up of products in the different electro-flow cells.

### 1.3. C–O Bond Formation

Oxidation of the very unreactive C–H (sp<sup>3</sup>) bond is a highly challenging task. There are many organometallic catalytic approaches to oxidize the unreactive C–H bond.<sup>[67–69]</sup> Pierce et al. describe hydroxylation of aliphatic C–H bond in



**Scheme 17.** Methods for 4-(Sulfonylmethyl)isoquinoline-1,3(2H,4H)-dione synthesis.<sup>[65]</sup>



**Scheme 18.** Electrolysis Conditions of Dehydrogenative Homocoupling of 55.<sup>[66]</sup>

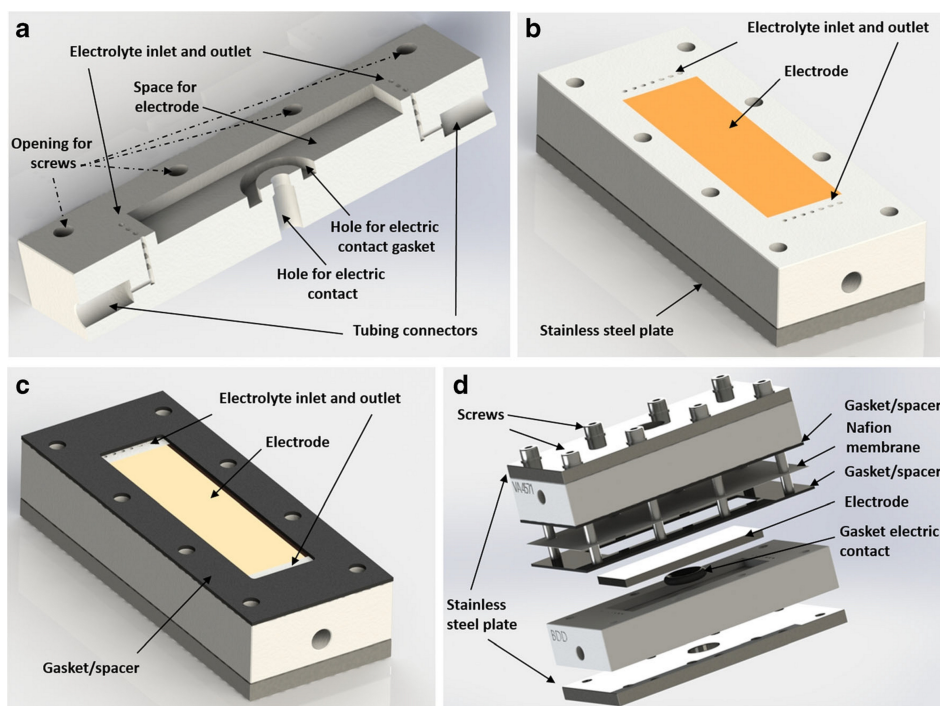


**Figure 13.** Technical drawings of 2 cm × 6 cm flow electrolysis cell: **a** Cross-section of the Teflon piece with connection for tubing, inlet, outlet, and free space for the electrode. **b** Complete half-cell containing Teflon piece, the electrode (yellow), and a stainless-steel plate. **c** Half-cell with gasket/ spacer on top. **d** Exploded drawing of a complete divided flow electrolysis cell. For the undivided mode.<sup>[66]</sup>

**Table 1.** Comparison of optimized conditions for different electrolysis cells.<sup>[66]</sup>

Cell type	Solvent	Applied charge Q[f]	Temp (°C)	Current density J[MA/cm <sup>2</sup> ]	Electrode material	Flow rate (mL/min)	Yield (%)	Production (g/min)
Batch (25 mL)	HFIP + 15 Vol% H <sub>2</sub> O	1.2	50	6.1	GC/GC	–	46	0.002
2 × 6cm flow	HFIP	1.0	10	60	BDD/SS	2.24	62	0.3
4 × 12 cm flow	HFIP	1.0	10	60	BDD/SS	8.95	58	1.3
EUT pilot cell	HFIP	1.0	0	40	BDD/SS	38.8	59	16.9

Supporting electrolyte for batch is Et<sub>4</sub>NBr (0.8 mol/L), and for flow and EUT pilot cell is MeBu<sub>3</sub>NO<sub>3</sub>SOMe (0.005 mol/L).

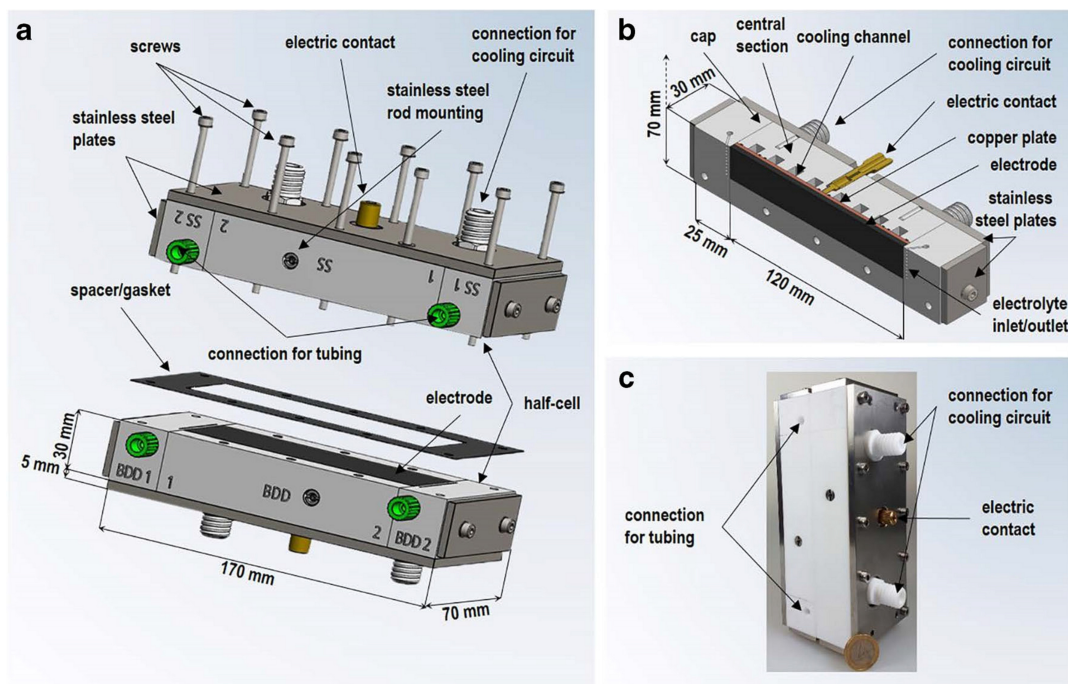


**Figure 14.** Technical drawings of 4 cm × 12 cm flow electrolysis cell. **a** Partly exploded drawing of the full-featured flow cell. **b** Cross-section of one half-cell. **c** Completely mounted 4 cm × 12 cm flow electrolysis cell and a Euro coin (diameter: 23.25 mm) for comparison.<sup>[66]</sup>

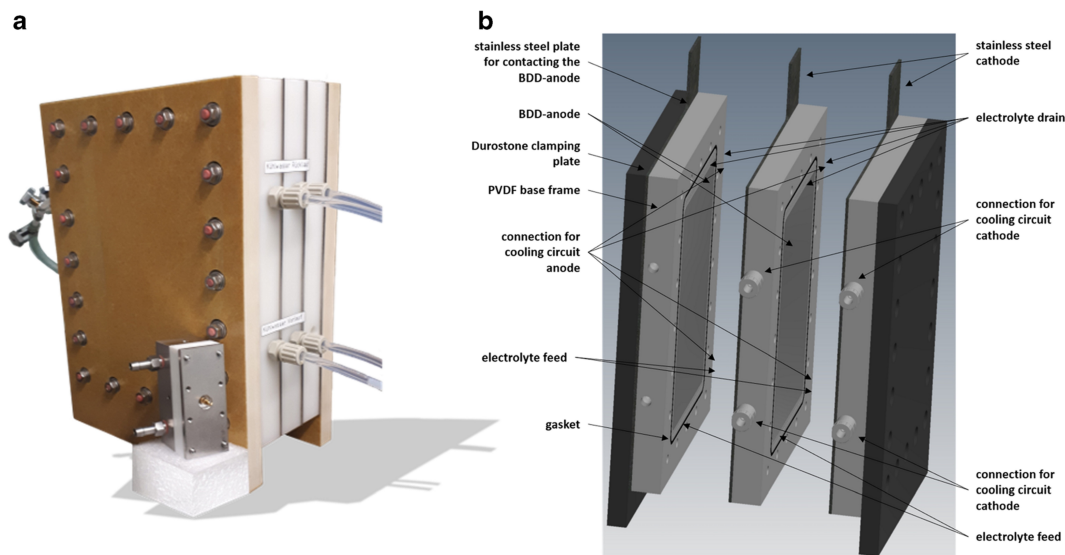


**Figure 15.** EUT pilot cell: **a** EUT pilot cell with 2 cm × 6 cm flow electrolysis cell for size comparison. **b** Technical drawing of three Polyvinylidene fluoride (PVDF) frames with inserted BDD electrodes, cooling connections, electrolyte feed, and gaskets.<sup>[66]</sup>

presence of organometallic complexes and ketone as catalyst<sup>[68]</sup> Jiang et al described the visible-light induced oxidation of  $sp^3$  C–H bonds to ester and ketone.<sup>[70]</sup> In summary oxidation of the C–H bond is commonly achieved by highly expensive reagents in multistep reactions but, using electrochemical

technology we can achieve the reaction in an exceedingly simple fashion. Continuous flow electrochemical transformation provides an increased electrode surface ratio that helps to achieve a high product ratio.<sup>[42]</sup>

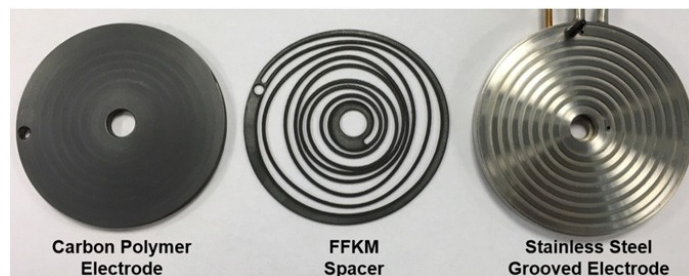
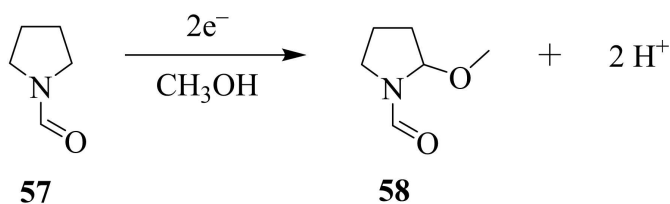


**Figure 16.** Components of the extended channel length microflow electrolysis cell.<sup>[71]</sup>

Green et al. designed a microreactor having an extended spiral electrolyte channel to study the rate of methoxylation of *N*-formylpyrrolidine **57**<sup>[71]</sup> (Scheme 19). Carbon filled polyvinylidene fluoride (C/PVDF) disc as anode and circular 316 L stainless steel plate act as cathode. The spiral electrolyte channel is created with a spiral spacer that permits the flow of reactants in between electrodes. The length of the electrolyte channel is 1000 mm and 2 mm in width (Figure 16). Different concentrations of the *N*-formylpyrrolidine were used for methoxylation with different cell current and flow rates of range 0.25 to 3.0 cm<sup>3</sup>min<sup>-1</sup>. It is reported that repeated use at a flow rate of 0.25 cm<sup>3</sup>min<sup>-1</sup> at electrolyte concentration 0.05 M and 0.1 M of reactant concentration yield 0.99 fractional conversions. The fractional conversion rate of reactants at different parameters is summarized in (Table 2).



**Scheme 19.** Methoxylation of *N*-formylpyrrolidine.

**Table 2.** Fractional conversion rate at different parameter.<sup>[71]</sup>

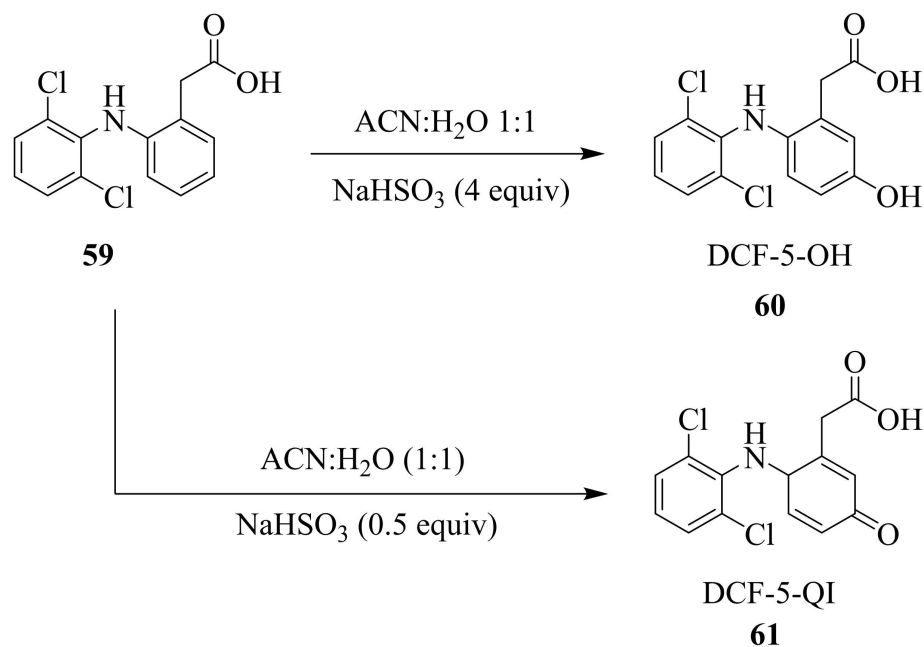
Concentration of reactant	Flow rate (cm <sup>3</sup> min <sup>-1</sup> )	Cell current (A)	Fractional conversion	Fractional selectivity	Product formation rate (g h <sup>-1</sup> )
0.1	0.25	0.1	0.99	0.88	0.17
	0.5	0.2	0.99	0.95	0.37
	1.0	0.4	0.86	0.95	0.64
	2.0	0.8	0.86	0.94	1.26
	3.0	1.5	0.88	0.91	1.86
0.5	0.25	0.5	0.96	0.89	0.82
	0.5	1.0	0.95	0.87	1.60
	1.0	2.0	0.93	0.88	3.16

Stalder et al.<sup>[72]</sup> used 5 drugs to test the continuous flow electrochemical oxidation that are, albendazole, diclofenac, tolbutamide, primidone, and chlorpromazine.<sup>[72]</sup> DCF (Diclofenac) **59** 0.1 M solution was prepared in (acetonitrile and water at 1 : 1 ratio) solution. The solution mixture was flowing in the presence of a constant current of 113 mA. The flow rate was decreased from 0.235 mL/min to 0.088 mL/min. DCF-5-OH **60** was formed up to 46% with quinone imine derivative DCF-5-QI **61** (Scheme 20).<sup>[72]</sup>

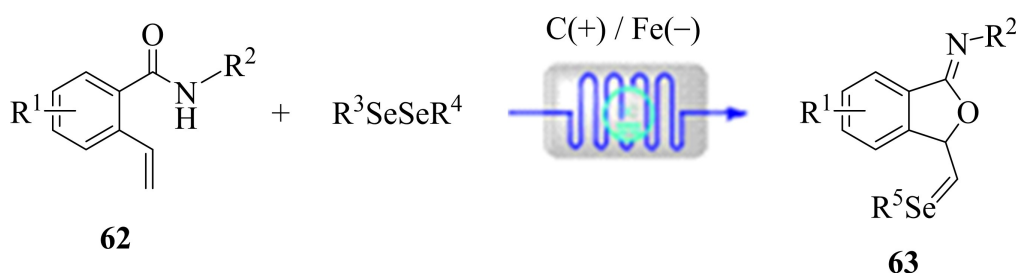
Bian et al.<sup>[73]</sup> explain the synthetic approach of selenium-substituted imino-isobenzofuran **63** using 2-vinylbenzanmides **62** and diselenides in continuous electrochemical microreactor.<sup>[73]</sup> (Scheme 21). The electro flow microreactor consists of cannon anode (50×50×0.5) mm and iron plate cathode (50×50×1) mm. The volume of the microflow tube is 1 mL. Mixture of 2-vinyl benzamide (0.2 mM, 1.0 equivalent), diselenide (0.1 mM, 0.5 equivalent) and lithium perchlorate (0.1 mM, 0.5 equivalent) dissolved with ACN and subjected to microreactor chamber by providing 15 mA current flow with flow rate of 225 μL/min. The percentage yield was formed quite attractive in different substituted benzamides.

Compounds containing C–O bond, for instance, esters, are successfully synthesized through carboxylate activation.<sup>[68]</sup> However, due to less atom economy, use of toxic reagents, waste generation, and drastic reaction conditions, other methods have been studied as an alternative approach.<sup>[69]</sup> Diederich and co-workers,<sup>[74]</sup> for the first time, applied an anodic oxidation approach for the conversion of Breslow intermediate **66** (formed by the reaction of *N*-heterocyclic carbene **65** with aldehyde) to intermediate **67** which reacts with an alcohol to give ester **68** (Scheme 22).

Green et al.<sup>[75]</sup> designed an undivided microfluidic electrolytic batch cell for oxidative esterification of aldehydes in the presence of catalyst *N*-heterocyclic carbene (NHC). They performed oxidative esterification of methyl 4-formylbenzoate **70** with methanol. Aldehyde **70**, MeOH, thiazolium salt **69**, and DMSO in THF were taken in reservoir 1 and 1,8-diazabicyclo[5.4.0]undec-7-ene (DBU) in THF was taken in reservoir 2. The solutions were introduced into a mixing T-



**Scheme 20.** Electro-flow Conversion of DCF to DCF-5-OH and DCF-5-QI.<sup>[72]</sup>



**Scheme 21.** Methoxylation of 2-Vinyl Benzamides in Presence of Diselenides.<sup>[73]</sup>

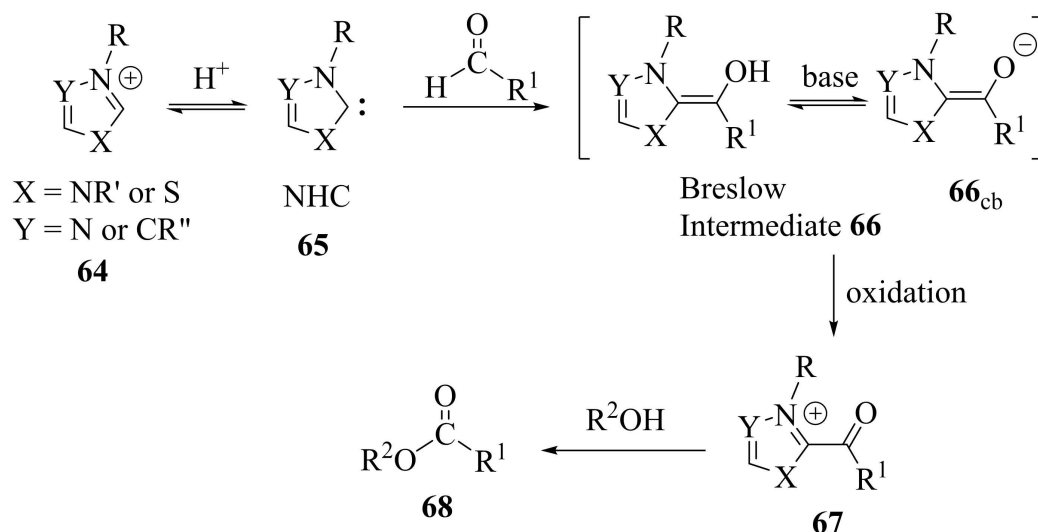
piece with a flow rate of  $0.5 \text{ mL min}^{-1}$ . This leads to the formation of Breslow intermediate **71** which was then oxidized to acylthiazolium **59** while passing through an electrolytic cell. The acylthiazolium **72** finally reacted with MeOH to yield 99% methyl ester **73** (Scheme 23).<sup>[75]</sup>

Kuleshova and co-workers<sup>[76]</sup> successfully performed methoxylation of *N*-formylpyrrolidine **74a** and 4-*t*-butyl toluene **75** by using a microfluidic electrolytic cell. Respectively, methoxylated products **74b** and **77** with new C–O bonds were prepared (Scheme 24). Schematics of the experimental setup are illustrated in (Figure 17). An electrolytic round cell with circular electrodes and a star-shaped channel pattern was designed. Anode was prepared from conductive carbon/polyvinylidene fluoride (PVDF) composite whereas cathode was prepared from stainless steel.<sup>[76]</sup>

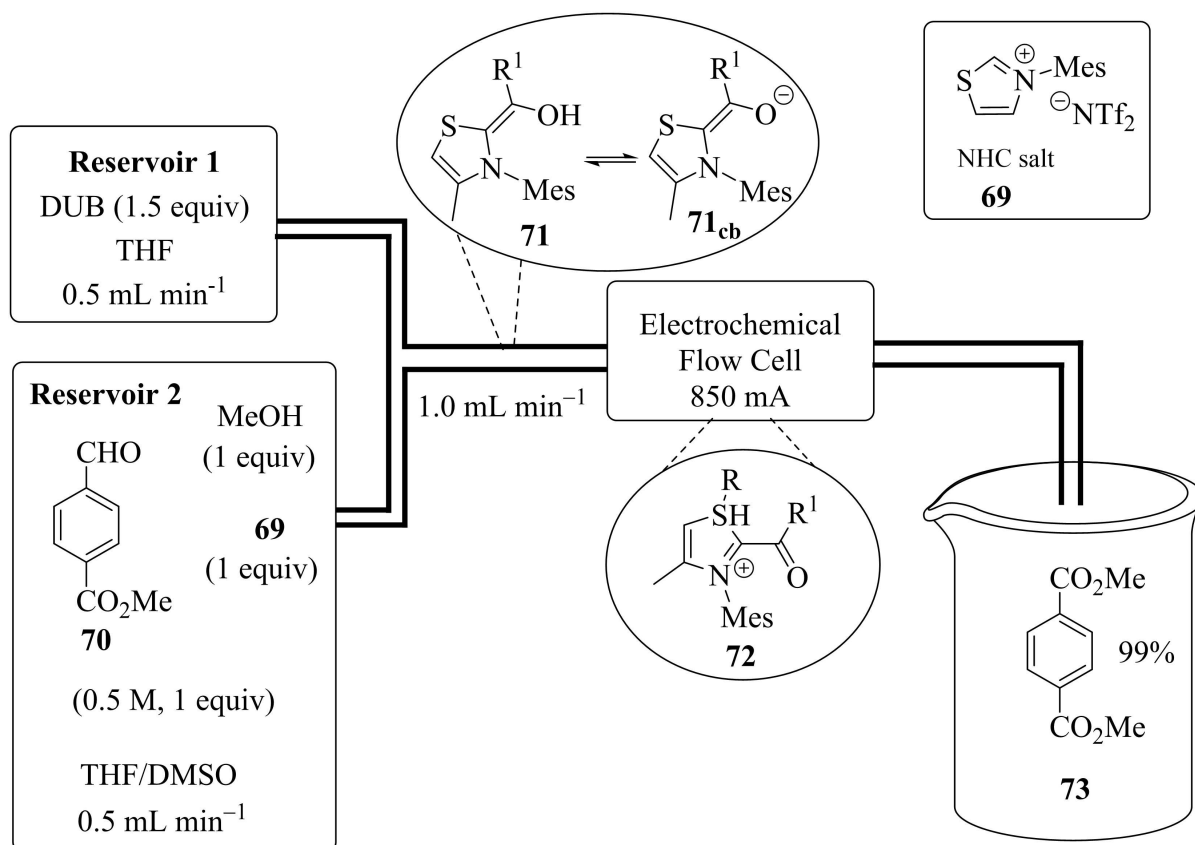
#### 1.4. C–I Bond Formation

Iodine is an essential trace element that is required by all living organisms, Iodine plays an important role in the endocrine system.<sup>[77]</sup> Organic compounds having iodine as functional groups are organic iodide. Several iodine-containing organic compounds have been found in seawater. Organic iodine in seawater is synthesized by macroalgae and phytoplankton.<sup>[78]</sup> Organic iodide also acts as an important reagent in organic synthesis. Zhdkankin et al.<sup>[79]</sup> reported that organic hypervalent iodine reagent attracts the interest of many researchers as an environmentally benign oxidant in organic synthesis. In this review, we discuss the electro-flow technique to synthesize the carbon-iodide functional group through C–H bond functionalization.

Watt et al.<sup>[79]</sup> describe the simple and efficient technique for the synthesis of diaryliodonium salt using the electro-



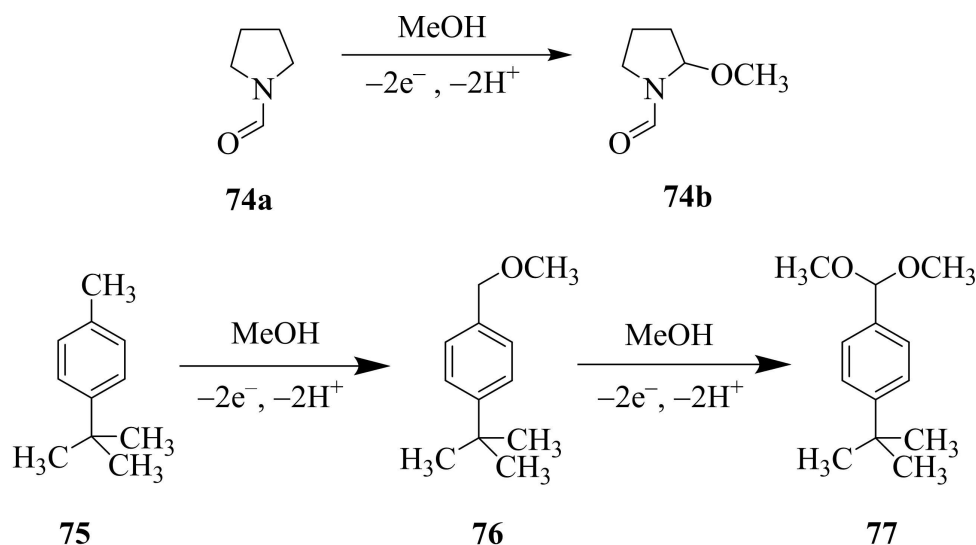
Scheme 22. NHC-Mediated oxidative esterification of aldehyde.<sup>[75]</sup>



Scheme 23. Flow-cell Arrangement for Oxidative Esterification of Aldehyde.<sup>[75]</sup>

chemical flow microreactor technique. In this mechanism, iodoarenes and alkyl substituted aromatic rings are coupled

using a microreactor. For the synthesis of iodine complex simple microreactor was designed, made up of two aluminum



**Scheme 24.** Methoxylation of *N*-Formylpyrrolidine and 4-*t*-Butyltoluene.<sup>[76]</sup>

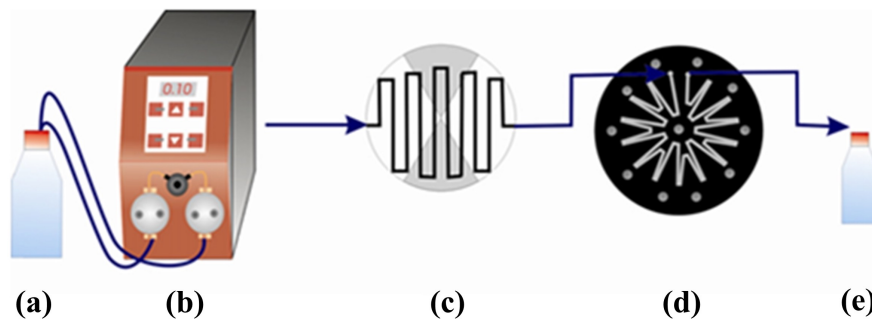
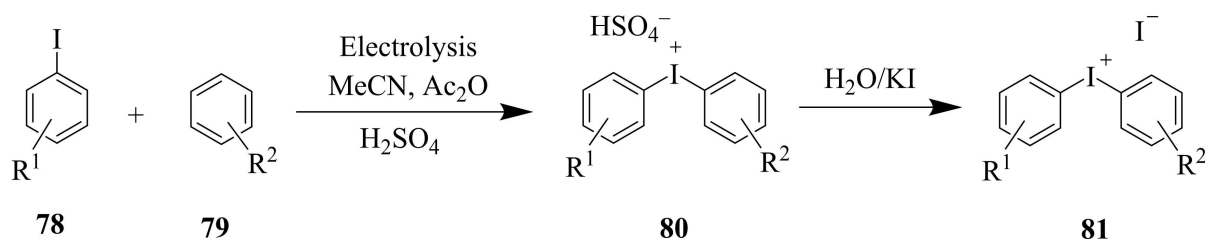


**Figure 17.** Schematic of the experimental setup, where (a) the solvent bottle, (b) pump, (c) ml sample loop, (d) microreactor, and (e) collection vial.<sup>[76]</sup>

bodies (50 mm diameter and 25 mm height). 0.1 mm thin platinum foil electrode-rod was constructed in the PTFE plates (35 mm diameter and 4 mm height). These electrodes were separated by FEP (fluorinated ethylene propylene) foil of variable thickness. FEP foil consists of a thin reaction channel (3 × 30 mm) with channel volume of 23  $\mu\text{L}$ . Diaryliodonium salt **81** was synthesized using the electrochemical microreactor

by reacting iodoarene and alkyl substituted aromatic compounds. Iodoarene **78** is oxidized at anode and forms a radical cation **80**, then this cation undergoes reaction with other arenes and forms an intermediate complex by losing electrons. Acetonitrile, sulfuric acid (2 M), and acetic anhydride were used as a solvent system for this reaction (Scheme 25). The amount of the product formation depends on so many factors



**Scheme 25.** Formation of Aromatic iodide by Microflow Technique.<sup>[79]</sup>

such as current supply, space between electrodes, the flow rate of the substrate, solvent system, etc. (Figure 18).<sup>[79]</sup>

Midorikawa et al.<sup>[80]</sup> describe the formation of the aromatic iodide by mono-iodination of the aromatic compound with electrochemically generated  $I^+$ . First of all, iodine radical was generated by oxidation of iodine in acetonitrile given  $CH_3CNI^+$  and  $I^+$  in platinum plate anode and platinum cathode under the constant current condition in H-type divide cells (Scheme 26). Reactive iodine species were characterized by cold spray ionization mass spectroscopy (CSI-MS). Micro mixing technique was used to mix the electrochemically generated  $I^+$  and 1,3-dimethoxy benzene using a microsystem consisting of a 1 mm single mixture having channel width 50  $\mu\text{L}$  and a microtube reactor 500  $\mu\text{L} \times 2\text{ m}$  at  $0^\circ\text{C}$  results in better mixing performance. This yields about 78% of the monoiodo aromatic compound **84**.<sup>[80]</sup>

### 1.5. C–N Bond Formations

Conventional methods used for C–H bond activation and generation of new C–N bond rely exclusively on expensive catalysts as well as the use of stoichiometric toxic oxidants. Generally, reactions are performed at elevated temperatures. Electrochemical flow reactions have now become a very strong and sustainable strategy for the construction of challenging carbon-nitrogen bonds. This review depicts the overview of C–N bond formation strategies. N-containing compounds are famous entities in natural products chemistry. Chemists have developed various conventional C–N bond formation platforms. However, such techniques require elevated temperature. To overcome this problem, the development of electrochemical methodologies has been examined.<sup>[7]</sup>

Electrochemical oxidation allows a powerful and important alternative and also shows unique reaction selectivity compared

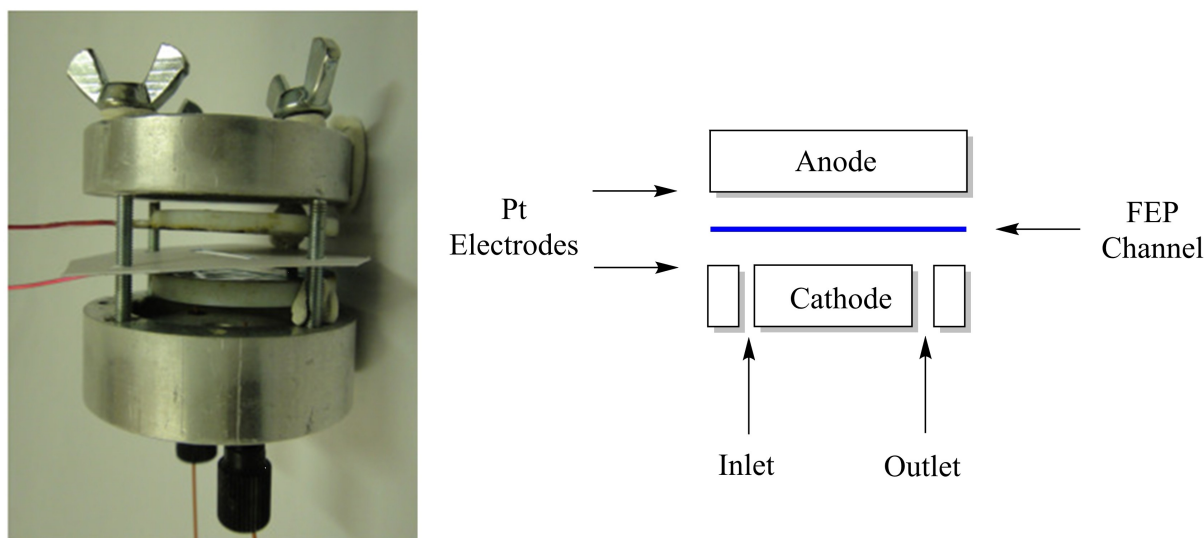
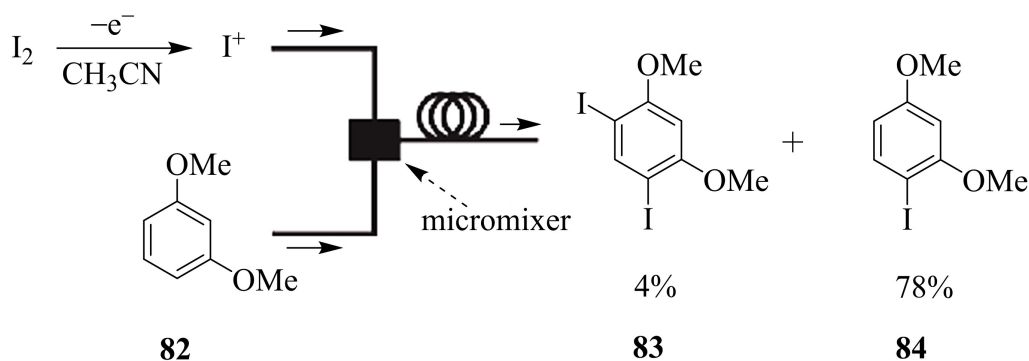
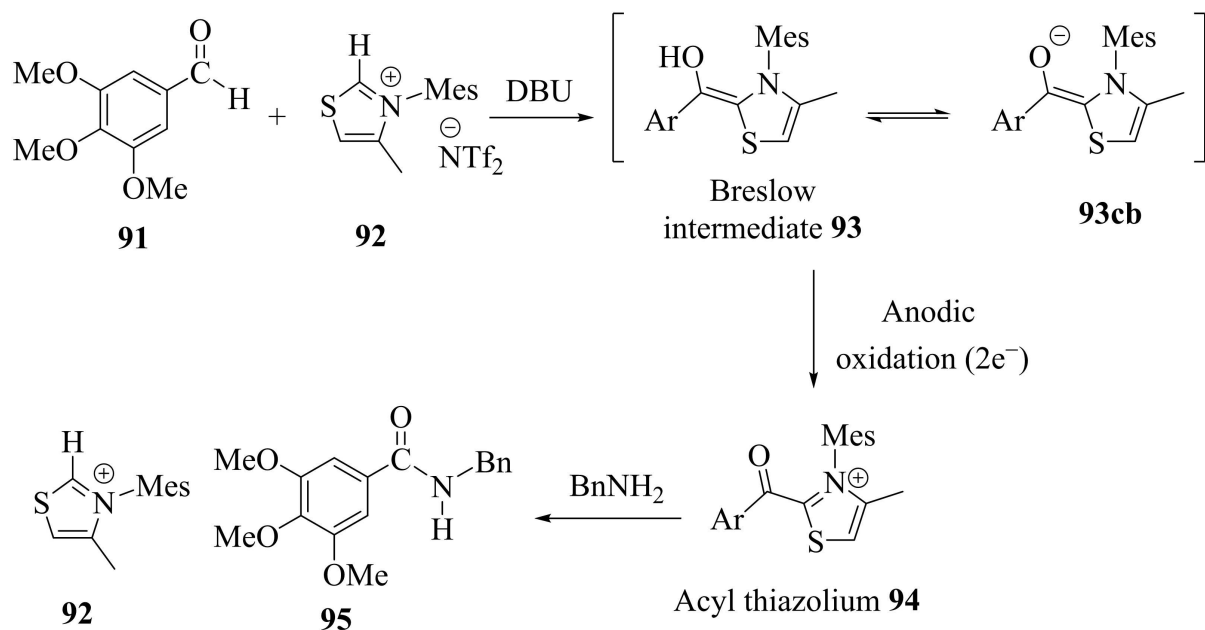


Figure 18. Electrochemical microreactor for CI bond formation.<sup>[79]</sup>

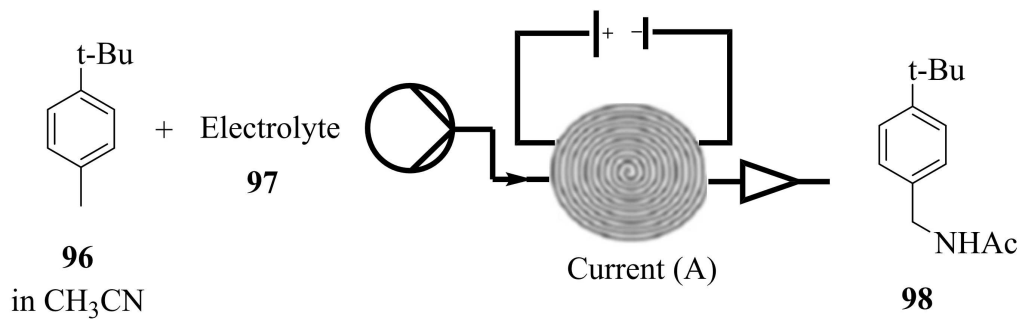


Scheme 26. Formation of Aromatic Iodide Using a Microreactor.<sup>[80]</sup>





**Scheme 29.** Electrosynthesis of Amide **95** from Aldehyde **91** Mediated by Thiazolium Bistriflimide **92**.<sup>[82]</sup>



**Scheme 30.** Anodic Oxidation of *p-t*-Butyltoluene in Acetonitrile.<sup>[83]</sup>

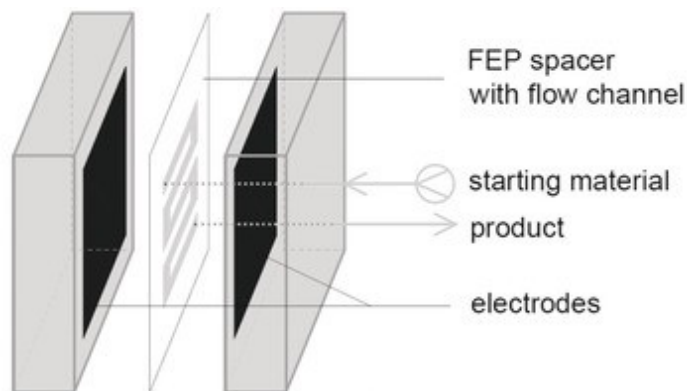
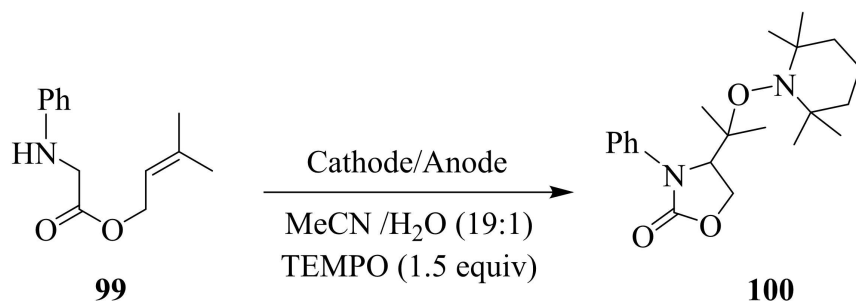


**Figure 19.** Electrochemical flow reactor: schematic diagram.<sup>[29]</sup>

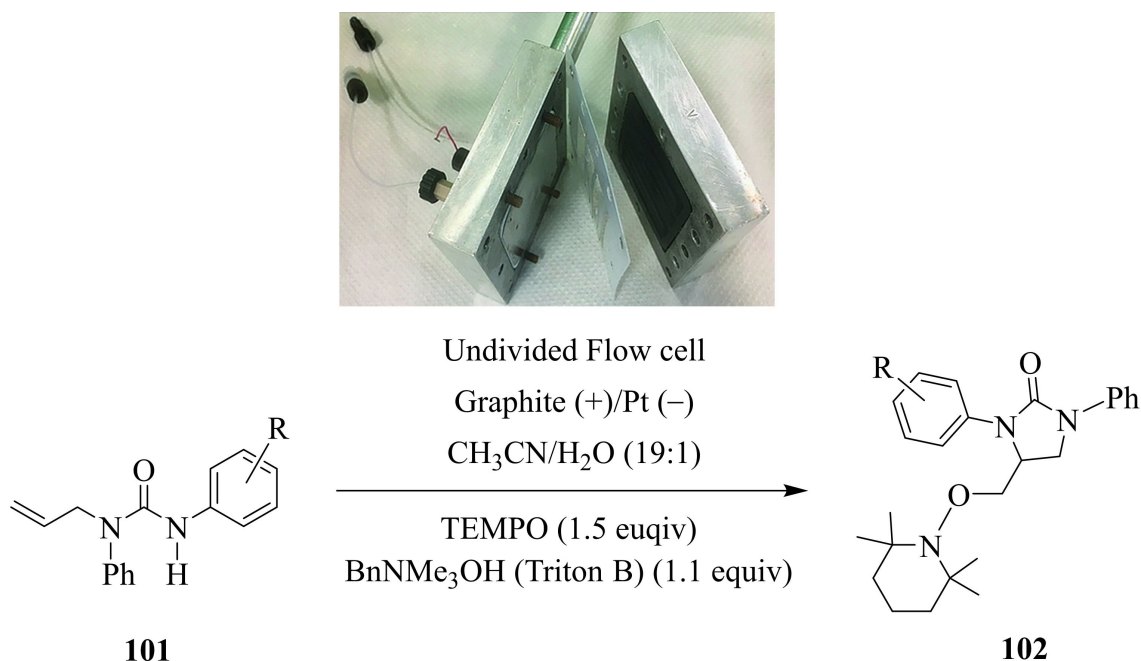


**Scheme 31.** Cyclization of Carbamates.<sup>[29]</sup>

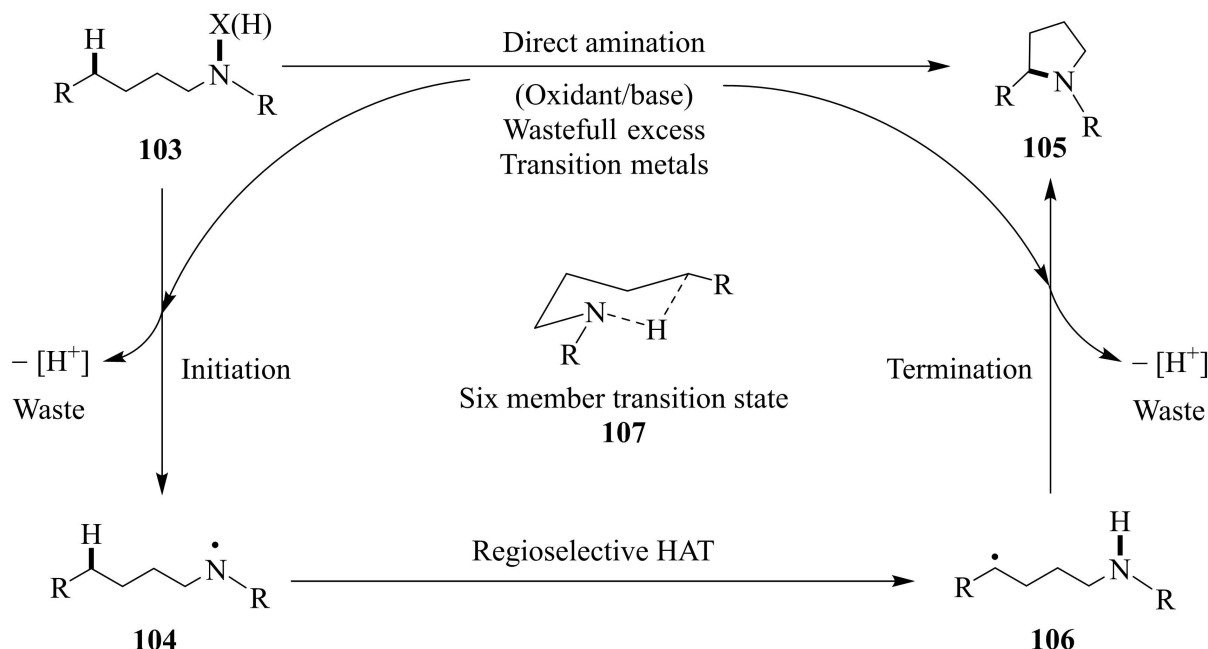
bond. To achieve high productivity and efficiency, the researchers tried to perform similar reactions by their flow methodology by replacing the inorganic base  $\text{Na}_2\text{CO}_3$  with the organic base Triton B. The allyl-substituted urea derivatives **101** which act as substrate was easily synthesized from mono-allyl aniline and isocyanates. Cyclic ureas **102** was synthesized from substrate **101** using graphite as anode and platinum cathode electrode with the current flow of 3F in flow electrochemical microreactor. The reaction was performed on their specialized reactor in which flow rates could be easily varied (Scheme 32).<sup>[85]</sup>

Further, Nikolaienko and co-workers<sup>[86]</sup> have developed an electrochemical intramolecular C–H amination. Several valuable pyrrolidines were obtained in good yields and with enhanced chemo-selectivity. Pyrrolidines rings were the major

entities in the five of eight anti-infective drugs approved in 2016 including anti-hepatitis C drug. Organic electrochemistry can be used to minimize the total energy losses and reduce waste production and ultimately decrease the overall cost of industrial synthesis. In that way, Nikolaienko and co-workers<sup>[86]</sup> used this technique with subsequent 1,5-HAT (1,5-hydrogen atom transfer) to overcome the problem faced during  $\text{C}(\text{sp}^3)\text{--H}$  amination and gave the standard protocol. The reaction was applied in either case of batch and continuous flow techniques and there was a better result in the case of the continuous flow method (Scheme 33).<sup>[86]</sup>



**Scheme 32.** Flow Electrochemical Synthesis of Cyclic Ureas.<sup>[85]</sup>



**Scheme 33.** Regioselective Intramolecular C(sp<sup>3</sup>)-H Bond Amination.<sup>[86]</sup>

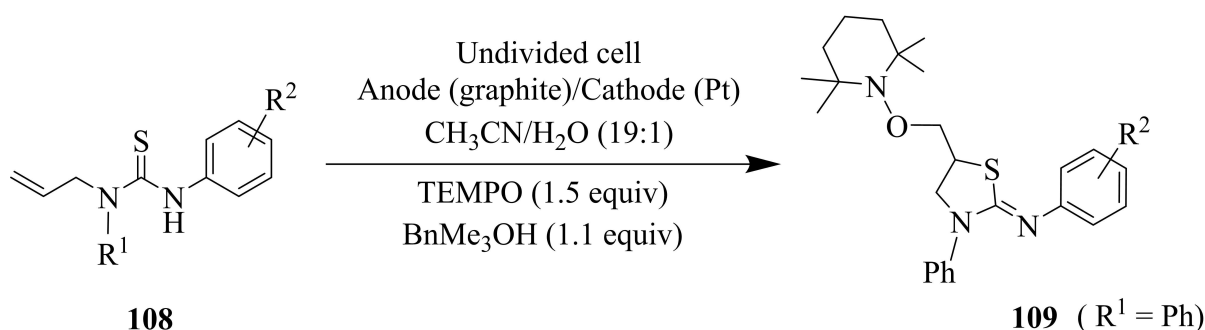
### 1.6. C-S Bond Formation

Electrochemical flow in organic synthesis is a sustainable approach to introduce the functional group. Electrolysis reaction in flow cells also helps to synthesize biologically important sulfur-containing compounds. Islam et al.<sup>[87]</sup> comparatively studied the effectivity of batch and electron flow techniques to synthesize thiazolidine-2-imine. *N*-allyl thio-urea **108** was taken as the standard starting material (Scheme 34). Batch electrolysis was tested using graphite electrode as anode and platinum electrode as a cathode, with a constant current of 10 mA. CH<sub>3</sub>CN:H<sub>2</sub>O (19:1) was used as the solvent in the electro-flow system. 35% product was formed due to the incomplete product conversion in batch

electrolysis. Then another reaction at the same concentration of reagent at 60°C in three-necked round bottom flasks was equipped with graphite electrode as anode and platinum as a cathode. 62% product conversion was observed; however, the product conversion was not sufficient.<sup>[87]</sup>

The reaction was transferred in the electro-flow setup (Figure 20). The substrate was used at a concentration of (0.025 M) with a capping agent at a similar solvent ratio at a flow rate of 0.2 mL/min. Electrolysis was carried out at 1.0–3.0 F electricity, however full conversion of the product takes place at the electricity of 3.0 F.<sup>[87]</sup>

Huang et al.<sup>[91]</sup> studied the effective dehydrogenative C-S cross-coupling reaction in flow electrolysis. Electrochemical C-S cross-coupling by evolving H<sub>2</sub> is an effective method to



**Scheme 34.** Electro-Flow Technique to Synthesize Thiazolidine-2-imine.<sup>[87]</sup>

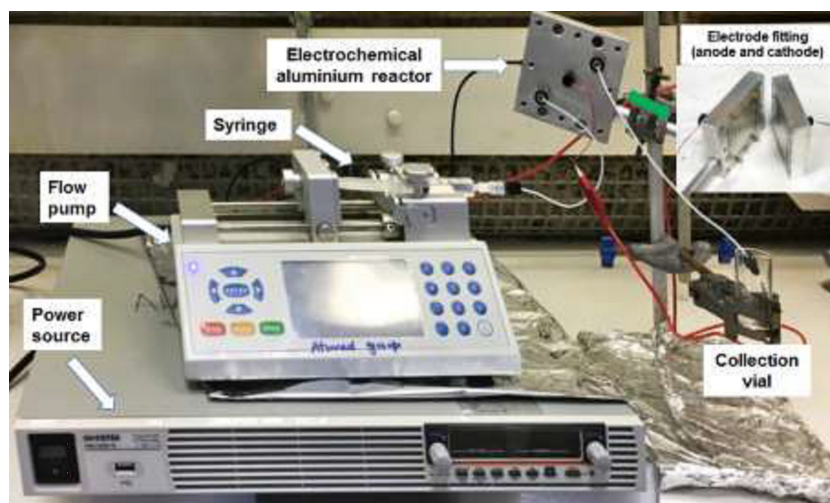


**Figure 20.** Electrochemical flow setup; aluminum reactor, flow pump, power source, syringe, and collection vial (for flow reactions, FEP film of 500  $\mu\text{m}$  thickness was used).

introduce the C–S bond in organic reaction.<sup>[88]</sup> An electro flow cell was designed with a platinum cathode and C/PVDF anode (Figure 21).

Due to the high electrochemical stability and low overpotential for reduction platinum foil was used as cathode. The reaction condition was set up as a flow rate of 0.3 mL/min and an electrical field of 35 mA for 24 hour. Mix solvent of MeCN:TFA (9:1) in presence of  $\text{Sc}(\text{OTf})_3$  (0.3 equiv) were used. In this condition, 1,4-benzoxanthines were synthesized by intermolecular dehydrogenation of C–S coupling (Scheme 35).

Folgueiras-Amador et al.<sup>[89]</sup> studied the electrochemical synthesis of the thiazolo [4,5-C] quinolone **113** from (N-(quinoline-3-yl) butanethioamide) **112** (Scheme 36). The flow electrolysis consists of platinum as cathode and graphite as anode with a surface area of 8.2  $\text{cm}^2$  each. A mixture of acetonitrile and methanol was used as a solvent. Electron flow was supported by a low current density of 0.49  $\text{mA cm}^{-2}$ . By increasing the substrate concentration and flow rate high product conversion can be obtained, (Table 3 represents the percentage of conversion of the product by changing different variables).

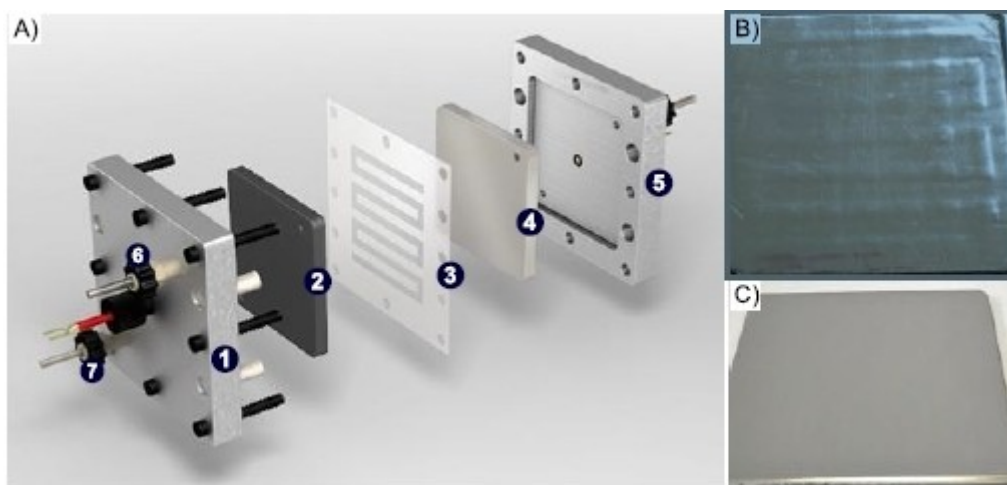
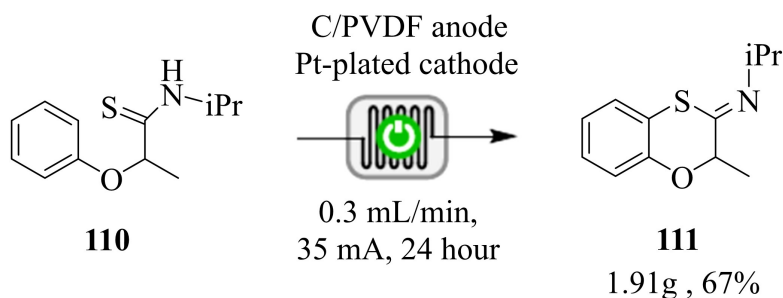
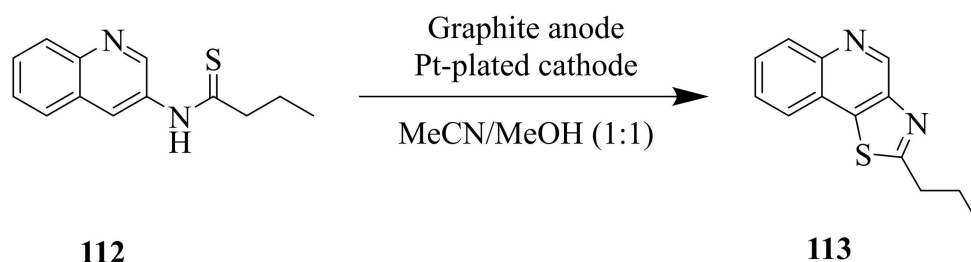


**Figure 21.** Design of the reactor and reaction scale-up. A) Design of an electrochemical flow cell. ① and ⑤: Electrode holder. ②: Anode. ③: Fluorinated ethylene propylene (FEP) foil. ④: Cathode. ⑥ and ⑦: Inlet and outlet. B) Pt foil electrode. C) Pt-plated electrode.<sup>[88]</sup>



Scheme 35. Electrolysis Using Cell Equipped with Pt Electrode.



Scheme 36. Aromatic Dehydrogenative C-S Bond Formation.

Table 3. Optimization of the reaction conditions.<sup>[89]</sup>

Entry	Concentration [mol L <sup>-1</sup> ]	Flow rate [mL min <sup>-1</sup> ]	Current density [mA cm <sup>-2</sup> ]	Current [F mol <sup>-1</sup> ]	<sup>1</sup> H NMR conversion [%]
1 <sup>[a]</sup>	0.025	0.05	0.49	2.0	33
2 <sup>[a]</sup>			0.98	4.0	50
3 <sup>[a]</sup>			1.46	6.0	98
4	0.025	0.05	1.46	6.0	> 99
5		0.1	2.93		> 99
6		0.2	5.85		> 99
7	0.05	0.2	11.71	6.0	> 99
8 <sup>[b]</sup>			4.88	2.5	> 99
9			3.90	2.0	90

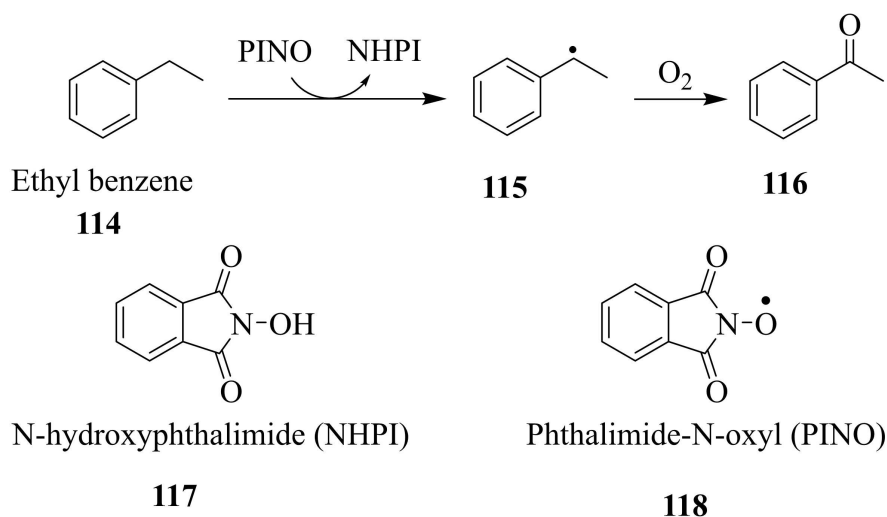
<sup>[a]</sup> 5 mol % of TEMPO. <sup>[b]</sup> 97 % isolated yield.

### 1.7. Benzylic Oxidation

The benzylic C-H bond is considered the center for the many useful and interesting transformations for preparing varieties of valuable compounds. The oxidation reaction is the most important reaction that can be performed on benzylic position and is heavily performed in synthetic chemistry.<sup>[90,91]</sup> Due to the massive importance of benzylic C-H oxidation reactions along with so many complications with the traditional method of such reactions, a new and more sophisticated methodology is always desirable. In this report, different successful strategies are discussed for such reactions based upon the electrochemical flow reactions. Mo and co-workers<sup>[92]</sup> have reported electro-

chemical reactions that were mediated in the air with *N*-hydroxyphthalimide (NHPI) **117** for the benzylic oxidation and then compared with the batch process simultaneously using varied reaction parameters. They developed new sustainable procedures that involve no metal and are compatible with heterocycles. Two decomposition mechanisms were observed i. e., reductive decomposition of NHPI and (Phthalimide-N-oxyl) PINO self-decomposition. To prevent reductive decomposition of NHPI at the cathode, a Nafion membrane was introduced to check the crossover of NHPI using the RVC electrode on either side. The mechanism of the reaction started with the abstraction of proton from the NHPI by pyridine followed by anodic electron transfer, which leads to PINO radical **118**. PINO facilitated the easy hydrogen abstraction from the benzylic compounds to give benzyl radical. The benzyl radical underwent decomposition in presence of molecular oxygen to yield a carbonyl compound. To check the self-decomposition of PINO radicals, the benzylic hydrogen abstraction rate was matched with the PINO radical generation by controlling the overpotential across the electrodes. The whole experiment was monitored using a cyclic voltammetry curve. Hence this study focused on the cost-effective RVC cathode in place of the platinum electrode and improved the slow kinetics of electrochemical flow reaction by the use of NHPI and gaseous molecular oxygen as co-oxidant for the benzylic oxidation reactions (Scheme 37).<sup>[92]</sup>

Another study conducted by Roth and co-workers<sup>[93]</sup> has developed a new tool in electro-organic synthesis for 4 or 6



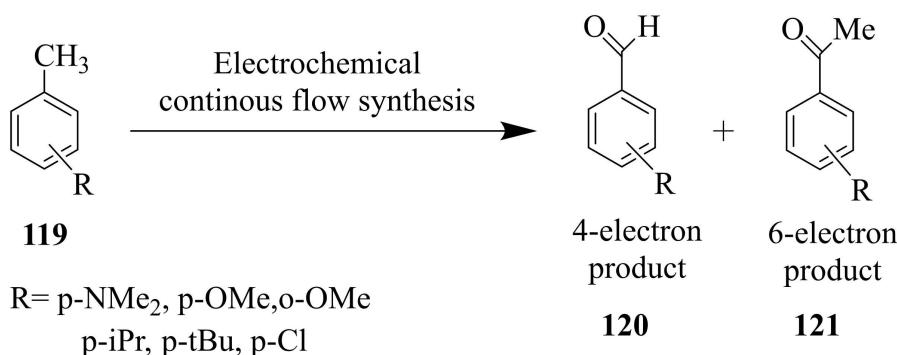
**Scheme 37.** Electrochemical Reaction for Benzylic Oxidation.<sup>[92]</sup>

electrons benzylic oxidation called a continuous-flow microfluidic-electrochemical device (flux module) (Scheme 38). They have used electron-rich substrate PMT (p-methoxy toluene) **119** and examined the microfluidic electrochemical reaction conditions.<sup>[93]</sup>

A systematic electrochemical cell used in the study was designed as a plate-based microfluidic cell (Figure 22). PMT was allowed to pass into the flux module at varied flow rates, and the products were monitored with the help of proton nuclear magnetic resonance (<sup>1</sup>H-NMR), liquid chromatography/mass chromatography (LC/MS). The effect of substituents in the substrate was also demonstrated using varied para substituents as shown in Table 4. The issue of reproducibility was also addressed by monitoring the product ratio.<sup>[93]</sup>

### 1.8. Biologically Active Molecules

Over the last two decades, there has been surplus advancement in the C–H functionalization strategies and the application of those technologies for the synthesis of complex targets like natural and pharmaceutical agents. The modification of the C–H bonds with transition metal-catalyzed form has made it possible to synthesize numerous biologically active molecules and natural products.<sup>[94–97]</sup> Such tools have the power to streamline multistep chemical processes by rendering functional group interconversion unnecessary. The synthetic approaches toward transition metal-catalyzed transformations at C–H bonds are divided into two categories: Outer sphere and inner sphere mechanisms.<sup>[98]</sup> The outer sphere mechanism occurs when there is the direct interaction of the C–H bond with the ligand coordinated with the central metal whereas the formation of a carbon-metal bond as a result of C–H bond



**Scheme 38.** Electro Benzylic Oxidation in Continuous Flow.<sup>[93]</sup>

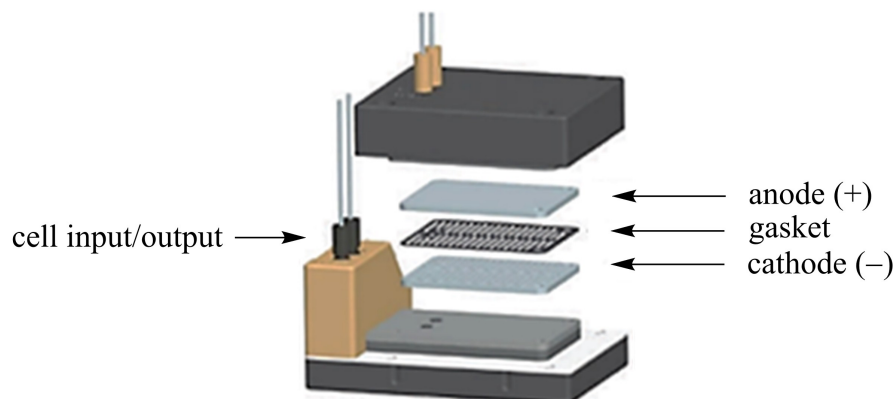


Figure 22. - Flux continuous flow electrochemistry module (flux module).<sup>[93]</sup>

Table 4. Substrate oxidation potentials and isolated yields for various tolyl substrates.<sup>[93]</sup>

Exp.	R-group	Oxidation peak potential (V) <sup>a</sup>	Electrons (F/mol)	Temp. (°C)	Aldehyde:ester isolated yield (%)
1	p-NMe <sub>2</sub>	0.83	3	0	21:0
2	p-OMe	1.66	7	65	0:62
3	p-tBu	2.11	8	65	38:0
4	p-OAc	2.14	8	65	n/a <sup>b</sup>
5	p-iPr	2.16	10	65	24:0:9 <sup>c</sup>
6	p-Cl	2.22	8	65	32:0
7	p-CN	2.52	8	65	n/a <sup>d</sup>
8	p-NO <sub>2</sub>	2.72	8	65	n/a <sup>d</sup>
9	o-OMe	n/a	7	65	3:0:10 <sup>c</sup>

<sup>a</sup> Obtained by cyclic voltammetry, vs. SCE. <sup>b</sup> Deacetylation occurs. <sup>c</sup> Isolated yields for aldehyde:ester:methoxy-aldehyde. <sup>d</sup> No oxidation.

cleavage leads to the formation of the inner-sphere mechanism. Here are some best examples of transition metal-metal

catalyzed biologically active molecules. Schipper et al.<sup>[99]</sup> were the leading researchers in C–H functionalization. they devised a new protocol for aryl C–H bond functionalization and demonstrated the power of this process for rapidly crafting modified arene and heteroarene derivatives.

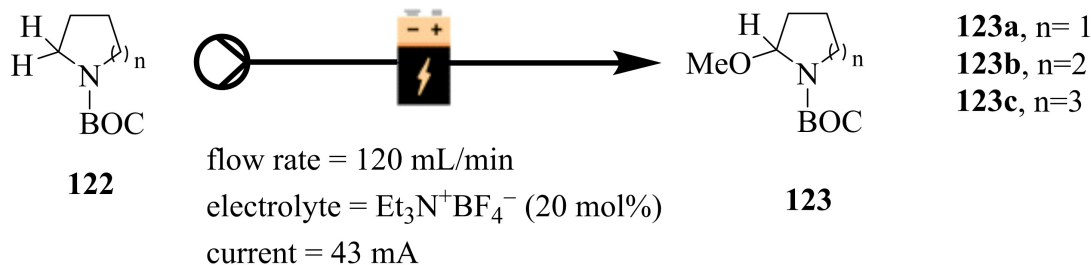
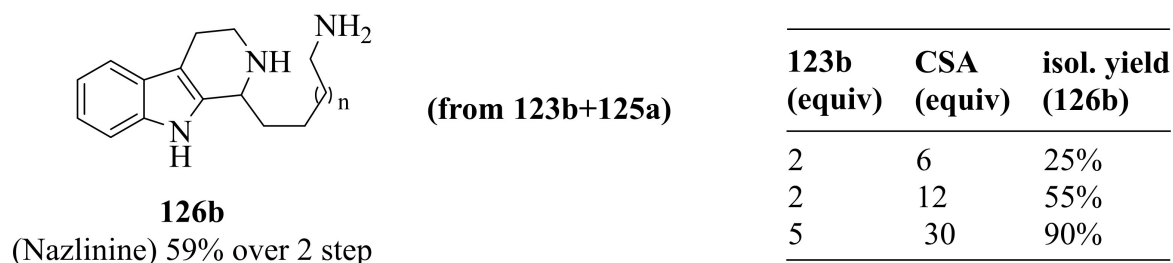
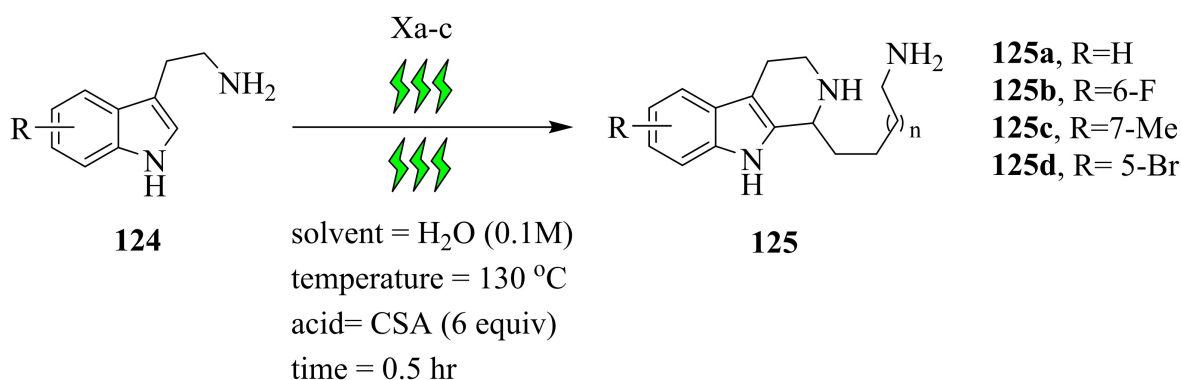
Flow electro-chemistry is a very beneficial tool to synthesize biologically active molecules. Kabeshov et al.<sup>[100]</sup> describe continuous flow electrochemistry as an enabling tool, that permits the direct preparation of a library of the indole alkaloids. Continuous flow conditions were applied to methoxylation at  $\alpha$ -position of cyclic amine (varying ring size) with N-protected pyrrolidine, piperidine, azepane, and morpholine.  $\alpha$ -methoxylation of cyclic amine followed by Pictet-Spengler reaction with tryptamine (two-step synthesis) (Figure 23), Nazlinine synthesized as product, and the yield percentage is 59% (Scheme 39).<sup>[100]</sup>

## 2. Conclusion and Perspective

Different examples and approaches represented in this review genuinely show the great usefulness of the electrochemical flow technique in the field of organic synthesis to functionalize C–H bonds. Electrochemical flow reactors overcome the



Figure 23. Two steps process for Nazlinine synthesis.<sup>[100]</sup>

**Step 1: Flow electrochemistry****Step 2 : Microwave irradiation****Scheme 39.** Continuous Flow Electrochemistry Approach to Synthesize Nazlinine Via Two Steps.<sup>[100]</sup>

limitation of different traditional techniques, by improving the C–H bond activation time and cost. Due to the environmentally benign, high surface-to-volume ratio, and attractive mass transports between phases, flow electrochemical technology is useful in organic synthesis. Besides many advantages, this method is used only in limited chemical and pharmacological industries due to the complex and expensive setup. One of the several challenges that limit the application of flow electrochemistry in the industrial field includes the formation of insoluble solids as the main product or side product which can cause a problem in uniform flow.<sup>[101]</sup> Moreover, during

electrochemical synthesis, different gases like  $\text{N}_2$  or  $\text{H}_2$  are produced that create a gas-liquid segment and affect the quality of the product. Further research and development of microreactors with easy setup and economic electrochemical flow microreactors will certainly contribute to the field commercialization of electro-flow techniques.

## Acknowledgment

Support from the Cardiff University to Dr. Nisar Ahmed is gratefully acknowledged. We would like to thank Dr. B. Shirinfar for valuable technical assistance and discussions.

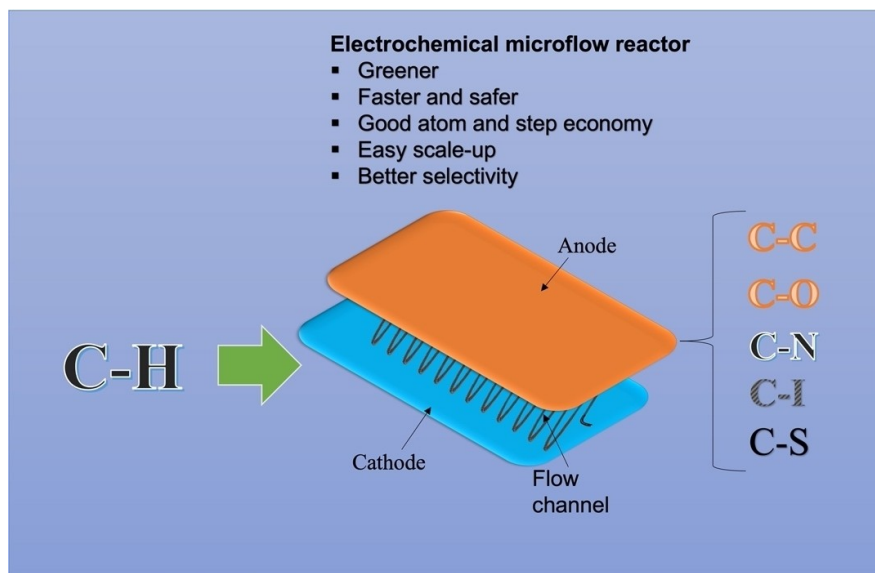
## References

- [1] J. A. Ellman, L. Ackermann, B.-F. Shi, *J. Org. Chem.* **2019**, *84*, 12701–12704, DOI: 10.1021/acs.joc.9b02663.
- [2] S. Govaerts, A. Nyuchev, T. Noel, *J. Flow Chem.* **2020**, *10*, 13–71.
- [3] X. Tang, X. Jia, Z. Huang, *Chem. Sci.* **2018**, *9*, 288–299, DOI: 10.1039/C7SC03610H.
- [4] J.-T. Yu, C. Pan, *Chem. Commun.* **2016**, *52*, 2220–2236, DOI: 10.1039/C5CC08872K.
- [5] H. M. L. Davies, J. D. Bois, J.-Q. Yu, *Chem. Soc. Rev.* **2011**, *40*, 1855–1856, DOI: 10.1039/C1CS90010B.
- [6] J. C. Lewis, P. S. Coelho, F. H. Arnold, *Chem. Soc. Rev.* **2011**, *40*, 2003–2021, DOI: 10.1039/c0cs00067a.
- [7] M. D. Kärkäs, *Chem. Soc. Rev.* **2018**, *47*, 5786–5865, DOI: 10.1039/C7CS00619E.
- [8] C. Perez-Rizquez, A. Rodriguez-Otero, J. M. Palomo, *Org. Biomol. Chem.* **2019**, *17* (30), 7114–7123, DOI: 10.1039/c9ob01091b.
- [9] X.-Q. Chu, D. Ge, Z.-L. Shen, T.-P. Loh, *ACS Catal.* **2018**, *8*, 258–271, DOI: 10.1021/acscatal.7b03334.
- [10] M. M. Díaz-Requejo, A. Caballero, M. R. Fructos, P. J. Pérez, *Alkane C–H Act. Single-Site Met. Catal.* **2012**, 229–264, DOI: 10.1007/978-90-481-3698-8\_6.
- [11] K. Wang, F. Hu, Y. Zhang, J. Wang, *Sci. China Chem.* **2015**, *58*, 1252–1265, DOI: 10.1007/s11426-015-5362-5.
- [12] J. He, M. Wasa, K. S. L. Chan, Q. Shao, J.-Q. Yu, *Chem. Rev.* **2017**, *117*, 8754–8786, DOI: 10.1021/acs.chemrev.6b00622.
- [13] L. Niu, J. Liu, X.-A. Liang, S. Wang, A. Lei, *Nat. Commun.* **2019**, *10*, DOI: 10.1038/s41467-019-08413-9.
- [14] R. H. Crabtree, *J. Chem. Soc. Dalton Trans.* **2001**, *17*, 2437–2450, DOI: 10.1039/B103147N.
- [15] B. A. Frontana-Uribe, R. D. Little, J. G. Ibanez, A. Palma, R. Vasquez-Medrano, *Green Chem.* **2010**, *12*, 2099–2119.
- [16] a) R. Francke, R. D. Little, *Chem. Soc. Rev.* **2014**, *43*, 2492–2521; b) G. M. Martins, G. C. Zimmer, S. R. Mendes, N. Ahmed, *Green Chem.* **2020**, *22*, 4849–4870; c) G. M. Martins, B. Shirinfar, T. Hardwick, A. Murtaza, N. Ahmed, *Catal. Sci. Technol.* **2019**, *9*, 5868–5881; d) G. M. Martins, B. Shirinfar, T. Hardwick, N. Ahmed, *ChemElectroChem.* **2019**, *6*, 1300–1315; e) N. Sbei, G. M. Martins, B. Shirinfar, N. Ahmed, *Chem. Rec.* **2020**, *20*, 1530–1552; f) N. Sbei, T. Hardwick, N. Ahmed, *ACS Sustainable Chem. Eng.* **2021**, *9*, 18, 6148–6169.
- [17] E. J. Horn, B. R. Rosen, P. S. Baran, *ACS Cent. Sci.* **2016**, *2*, 302–308.
- [18] H. Kolbe, *Justus Liebig's Ann. Chem.* **1849**, *69*, 257–294.
- [19] S. Santoro, F. Ferlin, L. Ackermann, L. Vaccaro, *Chem. Soc. Rev.* **2019**, *48*, 2767–2782, DOI: 10.1039/C8CS00211H.
- [20] S. Maljuric, W. Jud, C. O. Kappe, D. Cantillo, *J. Flow Chem.* **2020**, *10*, 181–190, DOI: 10.1007/s41981-019-00050-z.
- [21] T. Hardwick, N. Ahmed, *ACS Sustainable Chem. Eng.* **2021**, *9*, 4324–4340, DOI: 10.1021/acssuschemeng.0c08434.
- [22] C. Ma, P. Fang, T.-S. Mei, *ACS Catal.* **2018**, *8*, 7179–7189, DOI: 10.1021/acscatal.8b01697.
- [23] T. H. T. Myren et al., *Organometallics.* **2019**, *38*, 1248–1253, DOI: 10.1021/acs.organomet.8b00535.
- [24] S. Möhle, M. Zirbes, E. Rodrigo, T. Gieshoff, A. Wiebe, S. R. Waldvogel, *Angew. Chem. Int. Ed.* **2018**, *57*, 6018–6041, DOI: 10.1002/anie.201712732.
- [25] A. Wiebe, T. Gieshoff, S. Möhle, E. Rodrigo, M. Zirbes, S. R. Waldvogel, *Angew. Chem. Int. Ed.* **2018**, *57*, 5594–5619, DOI: <https://doi.org/10.1002/anie.201711060>.
- [26] A. J. Bard, R. W. Murray, *Proc. Natl. Acad. Sci. USA* **2012**, *109*, 11484–11486, DOI: 10.1073/pnas.1209943109.
- [27] H. Kolbe, *Justus Liebig's Ann. Chem.* **1849**, *69*, 257–294, DOI: <https://doi.org/10.1002/jlac.18490690302>.
- [28] D. Pletcher, R. A. Green, R. C. D. Brown, *Chem. Rev.* **2018**, *118*, 4573–4591, DOI: 10.1021/acs.chemrev.7b00360.
- [29] A. A. Folguez-Amador, K. Philipps, S. Guilbaud, J. Poelaker, T. Wirth, *Angew. Chem. Int. Ed. Engl.* **2017**, *56*, 15446–15450, DOI: 10.1002/anie.201709717.
- [30] T. Hardwick, N. Ahmed, *RSC Adv.* **2018**, *8*, 22233–22249, DOI: 10.1039/C8RA03406K.
- [31] J. Kristal, R. Kodym, K. Bouzek, V. Jiricny, J. Hanika, *Ind. Eng. Chem. Res.* **2012**, *51*, 1515–1524, DOI: 10.1021/ie200654c.
- [32] R. Horcajada, M. Okajima, S. Suga, J. Yoshida, *Chem. Commun.* **2005**, *10*, 1303–1305, DOI: 10.1039/B417388K.
- [33] N. Tanbouza, T. Ollevier, K. Lam, *iScience.* **2020**, *23*, 101720, DOI: 10.1016/j.isci.2020.101720.
- [34] J. P. Barham, B. König, *Angew. Chem. Int. Ed.* **2020**, *59*, 11732–11747, DOI: 10.1002/anie.201913767.
- [35] L. Zhang, L. Liardet, J. Luo, D. Ren, M. Grätzel, X. Hu, *Nat. Catal.* **2019**, *2*, 266–373, DOI: 10.1038/s41929-019-0231-9.
- [36] Y.-C. Wu, R.-J. Song, J.-H. Li, *Org. Chem. Front.* **2020**, *7*, 1895–1902, DOI: 10.1039/D0QO00486C.
- [37] J. Kobayashi, Y. Mori, S. Kobayashi, *Chem. Asian J.* **2006**, *1*, 22–35, DOI: 10.1002/asia.200600058.
- [38] A. Ziogas et al., *J. Appl. Electrochem.* **2009**, *39*, 2297–2313, DOI: 10.1007/s10800-009-9939-6.
- [39] V. Hessel, *Chem. Eng. Technol.* **2009**, *32*, 1655–1681, DOI: 10.1002/ceat.200900474.
- [40] T. Illg, P. Löb, V. Hessel, *Bioorg. Med. Chem.* **2010**, *18*, 3707–3719, DOI: 10.1016/j.bmc.2010.03.073.
- [41] J. Yoshida, A. Nagaki, D. Yamada, *Drug Discovery Today Technol.* **2013**, *10*, DOI: 10.1016/j.ddtec.2012.10.013.
- [42] T. Noël, Y. Cao, G. Laudadio, *Acc. Chem. Res.* **2019**, *52*, 2858–2869, DOI: 10.1021/acs.accounts.9b00412.
- [43] A. Adeyemi, J. Bergman, J. Brånalt, J. Sävmarker, M. Larhed, *Org. Process Res. Dev.* **2017**, *21*, 947–955, DOI: 10.1021/acs.oprd.7b00063.
- [44] B. Mahajan, T. Mujawar, S. Ghosh, S. Pabbaraja, A. Singh, *Chem. Commun.* **2019**, *55*, DOI: 10.1039/C9CC06127D.
- [45] J. Yoshida, *Chem. Rec.* **2010**, *10*, 332–341, DOI: 10.1002/tcr.201000020.

- [46] J. M. R. Narayanam, C. R. J. Stephenson, *Chem. Soc. Rev.* **2010**, *40*, 102–113, DOI: 10.1039/B913880 N.
- [47] M. H. Shaw, J. Twilton, D. W. C. MacMillan, *J. Org. Chem.* **2016**, *81*, 6898–6926, DOI: 10.1021/acs.joc.6b01449.
- [48] M.-C. Fu, R. Shang, B. Zhao, B. Wang, Y. Fu, *Science*. **2019**, *363*, 1429–1434, DOI: 10.1126/science.aav3200.
- [49] J. C. Theriot, C.-H. Lim, H. Yang, M. D. Ryan, C. B. Musgrave, G. M. Miyake, *Science*. **2016**, *352*, 1082–1086, DOI: 10.1126/science.aaf3935.
- [50] N. V. Tsarevsky, K. Matyjaszewski, *Chem. Rev.* **2007**, *107*, 2270–2299, DOI: 10.1021/cr050947p.
- [51] Y. Mo et al., *Science*. **2020**, *368*, 1352–1357, DOI: 10.1126/science.aba3823.
- [52] D. Leifert, A. Studer, *Angew. Chem. Int. Ed.* **2020**, *59*, 74–108, DOI: 10.1002/anie.201903726.
- [53] S. Momeni, D. Nematollahi, *Green Chem.* **2018**, *20*, 4036–4042, DOI: 10.1039/C8GC01727 A.
- [54] S. Momeni, D. Nematollahi, *J. Electroanal. Chem.* **2019**, *857*, DOI: 10.1016/j.jelechem.2019.113746.
- [55] W.-J. Kong, L. H. Finger, A. M. Messinis, R. Kuniyil, J. C. A. Oliveira, L. Ackermann, *J. Am. Chem. Soc.* **2019**, *141*, 17198–17206, DOI: 10.1021/jacs.9b07763.
- [56] K.-J. Jiao, Y.-K. Xing, Q.-L. Yang, H. Qiu, T.-S. Mei, *Acc. Chem. Res.* **2020**, *53*, 300–310.
- [57] Q. Yang, P. Fang, T. Mei, *Chin. J. Chem.* **2018**, *36*, 338–352.
- [58] E. Steckhan, *Angew. Chem. Int. Ed. Engl.* **1986**, *25*, 683–701.
- [59] H. Li, C. P. Breen, H. Seo, T. F. Jamison, Y.-Q. Fang, M. M. Bio, *Org. Lett.* **2018**, *20*, 1338–1341, DOI: 10.1021/acs.orglett.8b00070.
- [60] S. Suga, M. Okajima, K. Fujiwara, J. Yoshida, *J. Am. Chem. Soc.* **2001**, *123*, 7941–7942.
- [61] S. Suga, M. Okajima, K. Fujiwara, J. Yoshida, *QSAR Comb. Sci.* **2005**, *24*, 728–741.
- [62] S. Suga, D. Yamada, J. Yoshida, *Chem. Lett.* **2010**, *39*, 404–406.
- [63] D. Horii, T. Fuchigami, M. Atobe, *J. Am. Chem. Soc.* **2007**, *129*, 11692–11693, DOI: 10.1021/ja075180s.
- [64] Y. Qiu, A. Scheremetjew, L. H. Finger, L. Ackermann, *Chem. Eur. J.* **2020**, *26* (15), 3241–3246, DOI: 10.1002/chem.201905774.
- [65] J. Xu et al., *Org. Chem. Front.* **2020**, *7*, 3223–3228, DOI: 10.1039/D0QO00909 A.
- [66] M. Selt, B. Gleede, R. Franke, A. Stenglein, S. R. Waldvogel, *J. Flow Chem.* **2021**, *11* (2), 143–162, DOI: 10.1007/s41981-020-00121-6.
- [67] G. B. Shul'pin, *Comptes Rendus Chim.* **2003**, *6*, 163–178, DOI: 10.1016/S1631-0748(03)00021-3.
- [68] C. J. Pierce, M. K. Hilinski, *Org. Lett.* **2014**, *16*, 6504–6507, DOI: 10.1021/ol503410e.
- [69] A. Jutand, *Organic Electrochemistry*, ed. O. Hammerich and B. Speiser, CRC Press, Fifth Edition, Revised and Expanded, **2015**, 1393–1432, DOI: 10.1201/b19122.
- [70] L.-Y. Jiang et al., *Green Chem.* **2020**, *22*, 1156–1163, DOI: 10.1039/C9GC03727F.
- [71] R. A. Green, R. C. D. Brown, D. Pletcher, B. Harji, *Electrochem. Commun.* **2016**, *73*, DOI: 10.1016/j.electcom.2016.11.004.
- [72] R. Stalder, G. P. Roth, *ACS Med. Chem. Lett.* **2013**, *4*, 1119–1123, DOI: 10.1021/ml400316p.
- [73] M. Bian et al., *Org. Biomol. Chem.* **2021**, *19*, 3207–3212, DOI: 10.1039/D1OB00236H.
- [74] S. W. Tam, L. Jimenez, F. Diederich, *J. Am. Chem. Soc.* **1992**, *114*, 1503–1505, DOI: 10.1021/ja00030a069.
- [75] R. A. Green, D. Pletcher, S. G. Leach, R. C. D. Brown, *Org. Lett.* **2015**, *17*, 3290–3293, DOI: 10.1021/acs.orglett.5b01459.
- [76] J. Kuleshova, J. T. Hill-Cousins, P. R. Birkin, R. C. D. Brown, D. Pletcher, T. J. Underwood, *Electrochim. Acta* **2011**, *11*, 4322–4326, DOI: 10.1016/j.electacta.2011.01.036.
- [77] S. J. Crockford, *Integr. Comp. Biol.* **2009**, *49*, 155–166, DOI: 10.1093/icb/icp053.
- [78] R. Vogt, R. Sander, R. von Glasow, P. J. Crutzen, *J. Atmos. Chem.* **1999**, *32*, 375–395, DOI: 10.1023/A:1006179901037.
- [79] K. Watts, W. Gattrell, T. Wirth, *Beilstein J. Org. Chem.* **2011**, *7*, 1108–1114, DOI: 10.3762/bjoc.7.127.
- [80] K. Midorikawa, S. Suga, J. Yoshida, *Chem. Commun.* **2006**, *36*, 3794–3796, DOI: 10.1039/B607284D.
- [81] Q. Wang et al., *Chem. Sci.* **2020**, *11*, 2181–2186.
- [82] R. A. Green, D. Pletcher, S. G. Leach, R. C. Brown, *Org. Lett.* **2016**, *18*, 1198–1201.
- [83] M. A. Kabeshov, B. Musio, S. V. Ley, *React. Chem. Eng.* **2017**, *2*, 822–825.
- [84] N. Ahmed, S. Khatoun, *ChemistryOpen*. **2018**, *7*, 576–582, DOI: 10.1002/open.201800064.
- [85] N. Ahmed, A. Vgenopoulou, *SynOpen*. **2019**, *3*, 46–48.
- [86] P. Nikolaienko, M. Jentsch, A. P. Kale, Y. Cai, M. Rueping, *Chem. Eur. J.* **2019**, *25*, 7177–7184, DOI: 10.1002/chem.201806092.
- [87] M. Islam, B. M. Kariuki, Z. Shafiq, T. Wirth, N. Ahmed, *Eur. J. Org. Chem.* **2019**, *6*, 1371–1376, DOI: 10.1002/ejoc.201801688.
- [88] C. Huang, X.-Y. Qian, H.-C. Xu, *Angew. Chem. Int. Ed. Engl.* **2019**, *58*, 6650–6653, DOI: 10.1002/anie.201901610.
- [89] A. A. Folgueiras-Amador, X.-Y. Qian, H.-C. Xu, T. Wirth, *Chem. Eur. J.* **2018**, *24*, 487–491, DOI: 10.1002/chem.201705016.
- [90] A. J. Catino, J. M. Nichols, H. Choi, S. Gottipamula, M. P. Doyle, *Org. Lett.* **2005**, *7*, 5167–5170, DOI: 10.1021/ol0520020.
- [91] a) J. P. Barham, B. König, *Angew. Chem. Int. Ed.* **2020**, *59*, 11732–11747, DOI: 10.1002/anie.201913767; b) Oliva et al. *Adv. Synth. Catal.* **2021**, *363*, 1810–1834.
- [92] Y. Mo, K. F. Jensen, *Chem. Eur. J.* **2018**, *24*, 10260–10265, DOI: 10.1002/chem.201802588.
- [93] G. P. Roth, R. Stalder, T. R. Long, D. R. Sauer, S. W. Djuric, *J. Flow Chem.* **2013**, *3*, 34–40.
- [94] G. Dyker, *Angew. Chem. Int. Ed.* **1999**, *38*, 1698–1712.
- [95] K. Godula, D. Sames, *Science*. **2006**, *312*, 67–72.
- [96] F. Kakiuchi, N. Chatani, *Adv. Synth. Catal.* **2003**, *345*, 1077–1101.
- [97] V. Ritleng, C. Sirlin, M. Pfeffer, *Chem. Rev.* **2002**, *102*, 1731–1770.
- [98] R. H. Crabtree, *J. Chem. Soc. Dalton Trans.* **2001**, *17*, 2437–2450.



## REVIEW



*T. Pokhrel, B. B. K., R. Giri, A. Adhikari, N. Ahmed\**

1 – 38

### **C–H Bond Functionalization under Electrochemical Flow Conditions**

Technology-driven electrocatalysis using microreactors for typically inert C–H bonds functionalization to generate molecular complexity, will allow access various chemicals (such as medicinally relevant compounds, fine chemicals, and other valuable derivatives) in continuous,

scalable, and sustainable fashion. Flow electrochemistry would be a future enabling technology to handling challenging and difficult synthesis for medicinal and pharmaceutical process chemistry in an environmentally benevolent way.